



## Abstract

Ocean ecosystems are increasingly stressed by human-induced changes of their physical, chemical and biological environment. Among these changes, warming, acidification, deoxygenation and changes in primary productivity by marine phytoplankton can be considered as four of the major stressors of open ocean ecosystems. Due to rising atmospheric CO<sub>2</sub> in the coming decades, these changes will be amplified. Here, we use the most recent simulations performed in the framework of the Coupled Model Intercomparison Project 5 to assess how these stressors may evolve over the course of the 21st century. The 10 Earth System Models used here project similar trends in ocean warming, acidification, deoxygenation and reduced primary productivity for each of the IPCC's representative concentration pathways (RCP) over the 21st century. For the "business-as-usual" scenario RCP8.5, the model-mean changes in 2090s (compared to 1990s) for sea surface temperature, sea surface pH, global O<sub>2</sub> content and integrated primary productivity amount to +2.73 °C, -0.33 pH unit, -3.45 % and -8.6 %, respectively. For the high mitigation scenario RCP2.6, corresponding changes are +0.71 °C, -0.07 pH unit, -1.81 % and -2.0 % respectively, illustrating the effectiveness of extreme mitigation strategies. Although these stressors operate globally, they display distinct regional patterns. Large decreases in O<sub>2</sub> and in pH are simulated in global ocean intermediate and mode waters, whereas large reductions in primary production are simulated in the tropics and in the North Atlantic. Although temperature and pH projections are robust across models, the same does not hold for projections of sub-surface O<sub>2</sub> concentrations in the tropics and global and regional changes in net primary productivity.

## 1 Introduction

Over the past decades, the ocean has undergone large physical and biogeochemical modifications in response to human-induced global change, as revealed by a variety

**BGD**

10, 3627–3676, 2013

## Multiple stressors of ocean ecosystems in the 21st century

L. Bopp et al.

Title Page

Abstract

Introduction

Conclusions

References

Tables

Figures



Back

Close

Full Screen / Esc

Printer-friendly Version

Interactive Discussion



## BGD

10, 3627–3676, 2013

---

**Multiple stressors of ocean ecosystems in the 21st century**

L. Bopp et al.

---

[Title Page](#)
[Abstract](#)[Introduction](#)[Conclusions](#)[References](#)[Tables](#)[Figures](#)[Back](#)[Close](#)[Full Screen / Esc](#)[Printer-friendly Version](#)[Interactive Discussion](#)

of in-situ and remote sensing observations. These changes encompass ocean surface warming, changes in ocean salinity, modifications of density structure and stratification, as well as an increase in dissolved inorganic carbon concentrations and a decrease in seawater pH in response to ocean uptake of anthropogenic carbon (Doney, 2010).

5 These physical and chemical modifications (Bindoff et al., 2007) have the potential to affect marine organisms and ecosystems (Doney et al., 2012).

Temperature for instance has a fundamental effect on biological processes, as most biological rates (e.g. enzyme reactions) are temperature-dependent. Sea surface temperature has increased by about  $+0.7^{\circ}\text{C}$  over the last 100 yr (Bindoff et al., 2007).  
 10 Some organisms may be able to acclimate to temperature changes that do not push them outside of their optimal range, but rising temperatures this century could cause poleward shifts in species thermal niches and a decline in diversity as shown by Thomas et al. (2012) for tropical phytoplankton. In addition, rising ocean temperatures lead to increased ocean stratification and changes in ocean mixing and ventilation that could induce indirect effects, that in turn reduce subsurface dissolved  $\text{O}_2$  concentrations (Plattner et al., 2001) and supply of nutrients to the euphotic layer, increasing nutrient stress for phytoplankton (Bopp et al., 2001).

Sea surface pH has declined by about 0.1 pH unit since pre-industrial times (Bindoff et al., 2007). This decrease, along with other large-scale changes in seawater chemistry (increased dissolved  $\text{CO}_2$ , decreased carbonate ion concentrations) are referred to as anthropogenic ocean acidification and are a direct consequence of the oceanic absorption of  $\sim 30\%$  of the total anthropogenic emissions of carbon dioxide  $\text{CO}_2$  since 1750 (Sabine et al., 2004). These changes may have adverse effects on marine organisms. For instance, lower carbonate ion concentrations reduce calcification for many calcifying organisms (Hofmann et al., 2010), very high  $\text{CO}_2$  levels impose increased physiological stress on heterotrophic organisms (Pörtner et al., 2008) and may lead to decreased stress on autotrophic organisms through  $\text{CO}_2$  fertilization of photosynthesis, particularly for slow-growers such as diazotroths (Hutchins et al., 2007).

## Multiple stressors of ocean ecosystems in the 21st century

L. Bopp et al.

Title Page

Abstract

Introduction

Conclusions

References

Tables

Figures



Back

Close

Full Screen / Esc

Printer-friendly Version

Interactive Discussion



Reduced oceanic  $O_2$  have been reported for coastal areas in response to human-induced eutrophication (Gilbert et al., 2010), and for the open ocean as a consequence of two major processes: a warming-induced reduction in solubility and increased stratification/reduced ventilation (Helm et al., 2011). This reduction in  $O_2$ , referred to as ocean deoxygenation, between the 1970s and the 1990s amounts to a global average reduction of  $-0.93 \text{ mmol m}^{-3}$  (Helm et al., 2011). Most organisms are not very sensitive to  $O_2$  levels as long as concentrations are adequate. However, beyond a critical threshold referred to as hypoxia (below  $50\text{--}80 \text{ mmol m}^{-3}$  depending on taxa), many organisms start to suffer from several physiological stresses that could ultimately lead to death under extremely hypoxic conditions (Keeling et al., 2010).

In addition, net production of organic matter by phytoplankton (net primary production or NPP), which represents the first link in open-ocean marine food webs, may also be impacted by climate change and climate variability (Behrenfeld et al., 2006). Boyce et al. (2010) reported a global decrease of phytoplankton biomass of 1 % per year since 1900 based mostly on ocean transparency measurements. However, this result is debated and might arise from a temporal sampling bias (Ryckaczewski and Dunne, 2011). Observations also suggest an extension of oligotrophic gyres by  $\sim 15\%$  between 1998 and 2007 (Polovina et al., 2008). Conversely, Henson et al. (2011) emphasize that this trend cannot be unequivocally attributed to the impact of global climate change but may rather a result from the strong La Niña in 1998, and that a much longer time series is needed to distinguish a global warming trend from natural variability. Whether or not these changes in primary productivity are attributable to global warming, they are likely to be felt further up the food chain, with potential implications on marine resources (Pauly and Christensen, 1995; Nixon and Thomas, 2001).

Marine ecosystems are adapted to particular environmental conditions, temperature, pH,  $O_2$  and NPP are fundamental controlling factors, which, when changed, affect how an ecosystem will be altered. Several previous modeling studies used coupled climate-marine biogeochemical models to investigate how these stressors could evolve under climate change scenarios. Most of these modeling studies will be discussed here

when compared to our new results, but they all indicate large changes in these marine ecosystem stressors over the coming decades.

Using 13 ocean-only models, Orr et al. (2005) showed that global-mean surface pH could drop by 0.3–0.4 pH unit in 2100 under the IS92a scenario (similar to the RCP8.5 scenario used in our study). In this scenario, Southern Ocean surface waters become undersaturated with respect to aragonite as soon as year 2050. In 2100, aragonite undersaturation extends throughout the entire Southern Ocean and into the subarctic Pacific Ocean.

Coupled climate-marine biogeochemical models used over the past 15 yr all project a long-term decrease in the oceanic O<sub>2</sub> inventory in response to anthropogenic global warming (e.g. Sarmiento et al., 1998; Plattner et al., 2001; Bopp et al., 2002). In a recent intercomparison of seven earth system models, Cocco et al. (2012) found that the oceanic O<sub>2</sub> inventory would decline by 2 to 4 % in 2100 under SRES-A2, an earlier IPCC scenario similar to the RCP8.5 scenario used here.

Finally, most coupled climate-marine biogeochemical models also project a decline in NPP in the coming decades as a response to anthropogenic global warming (e.g. Bopp et al., 2001). In a recent model intercomparison study of four coupled models, Steinacher et al. (2010) reported a decrease in global mean NPP of 2–20 % by 2100 relative to preindustrial conditions in the SRES A2 emission scenario.

These physical and biogeochemical changes in temperature, pH, O<sub>2</sub> and NPP are known to interact with each other, potentially leading to synergistic effects (Gruber, 2011). Some of these synergistic effects occur at the regional and global scales, one example being the still-debated impact of ocean acidification on ocean deoxygenation. Using ocean biogeochemical models and a simple parameterization based on mesocosm experiments and relating C/N ratios of organic matter to CO<sub>2</sub> levels (Riebesell et al., 2007), Oschlies et al. (2008) and Tagliabue et al. (2011) showed that increasing dissolved CO<sub>2</sub> could induce large increases in sub-surface O<sub>2</sub> utilization, hence expanding the volume of suboxic waters. Synergistic effects also take place at the physiological level. Temperature and dissolved CO<sub>2</sub> may affect levels of tolerance to

**BGD**

10, 3627–3676, 2013

## Multiple stressors of ocean ecosystems in the 21st century

L. Bopp et al.

Title Page

Abstract

Introduction

Conclusions

References

Tables

Figures

◀

▶

◀

▶

Back

Close

Full Screen / Esc

Printer-friendly Version

Interactive Discussion



low-O<sub>2</sub> concentrations (Pörtner et al., 2004, 2007), whereas elevated CO<sub>2</sub> and lower O<sub>2</sub> levels may reduce thermal tolerance of some organisms (Pörtner 2010; Metzger et al., 2008). These studies emphasize that multiple stressors should be studied together simultaneously in order to be able to evaluate synergistic effects.

Here, we use the most recent simulations performed in the framework of the Coupled Model Intercomparison Project 5 (CMIP5, Taylor et al., 2012) to assess how these stressors may evolve over the course of the 21st century. We focus on four stressors: temperature, pH, O<sub>2</sub> and NPP, while comparing four different representative concentration pathways (RCPs) scenarios across 10 different Earth System Models (ESMs), all including a marine biogeochemical component. The remainder of the paper is organized as follows. Section 2 describes the models and the set of simulations used in this study. Section 3 presents the main results and a discussion, describing major evolution of the different stressors at the global scale, at the regional scale and relations between the stressors. Conclusions and perspectives follow in Sect. 4.

## 2 Methodology

### 2.1 Models and simulations

The latest generation of Earth System Models (ESMs) were used to carry out simulations within the framework of CMIP5 (Taylor et al., 2012). These simulations include 4 future scenarios referred to as RCPs (Moss et al., 2010; van Vuuren et al., 2011): RCP8.5, RCP6.0, RCP4.5 and RCP2.6. The RCPs are labeled according to the additional radiative forcing level in 2100 with CO<sub>2</sub> concentrations reaching 936, 670, 538 and 421 ppm respectively. RCP2.6 is also referred to as RCP3PD for “peak and decline”: the atmospheric CO<sub>2</sub> peaks at a concentration of 443 ppm in 2050 before declining in the second half of the 21st century.

The selection of the 10 models used for this study was based on the availability of all variables necessary to discuss the four stressors we focus on, i.e. temperature, pH, O<sub>2</sub>

**BGD**

10, 3627–3676, 2013

## Multiple stressors of ocean ecosystems in the 21st century

L. Bopp et al.

Title Page

Abstract

Introduction

Conclusions

References

Tables

Figures

◀

▶

◀

▶

Back

Close

Full Screen / Esc

Printer-friendly Version

Interactive Discussion



## BGD

10, 3627–3676, 2013

---

**Multiple stressors of ocean ecosystems in the 21st century**

L. Bopp et al.

---

[Title Page](#)
[Abstract](#)[Introduction](#)[Conclusions](#)[References](#)[Tables](#)[Figures](#)[Back](#)[Close](#)[Full Screen / Esc](#)[Printer-friendly Version](#)[Interactive Discussion](#)

and NPP. They were also selected on the requirements that at least one representative concentration pathway (RCP) was performed up to 2099. We used historical simulations from 1870 to 2005, all climate change scenarios (RCPs) from 2006 to 2099, and pre-industrial control simulations. Historical and climate change scenarios are forced not only by prescribed atmospheric CO<sub>2</sub>, but also by other greenhouse gases and aerosols concentrations, anthropogenic land use evolution, as well as by natural forcings such as solar and volcanic forcings. In case several ensemble members were run for the same scenario and with the same model, only the first member was used. Note that the simulations used here are simulations in which atmospheric CO<sub>2</sub> is prescribed (as in Jones et al., 2013), and not the ones, also performed with several of these Earth System Models, in which atmospheric CO<sub>2</sub> is explicitly computed from prescribed anthropogenic emissions and the simulated ocean and land carbon sources and sinks (as in Friedlingstein et al., 2013). We did not use these latter simulations, as different atmospheric CO<sub>2</sub> levels between the different models for the same scenario would have added another degree of complexity in our model intercomparison study.

Table 1 presents the ten models used for this study. Each includes representations of the general circulation and physics of the atmosphere and the ocean, as well as biogeochemical components, including a representation of the ocean carbon cycle as well as the lowest trophic level of marine ecosystems (i.e. phytoplankton). However, the models differ in many respects. Thus attributing the causes of differences between models to particular processes or parameterizations must be taken as educated guesses.

Atmospheric and ocean resolutions vary widely across the different models. Typical atmospheric horizontal grid resolution is  $\sim 2^\circ$ , but it ranges from  $0.94^\circ$  to  $3.8^\circ$ . Typical oceanic horizontal resolution is  $\sim 1^\circ$ , but it ranges from  $0.3^\circ$  to  $2^\circ$ . The numbers of vertical levels varies from 24 to 95 in the atmosphere and 31 to 63 in the ocean. All marine biogeochemical components are typical Nutrient Phytoplankton Zooplankton Detritus (NPZD) models, but with varying degrees of complexity, illustrated for instance by the number of phytoplankton functional groups explicitly represented (from 1 to 3, see Table 1).

## 2.2 Model output, model mean and robustness

In this study, we make use of the standard CMIP5 output from the Program for Climate Model Diagnosis and Intercomparison (<http://pcmdi3.llnl.gov/esgcet/home.htm>). We use output provided by the different models listed in Table 1 and available at the time of writing. Not all models have performed all RCP simulations.

The variables selected for this study are annual-mean 3-D temperature, salinity, meridional velocity, pH, O<sub>2</sub> as well as 2-D vertically-integrated NPP and export production of organic particles at 100 m. For models that did not provide pH fields to the database at the time of this writing (MPI-ESM-LR and HadGEM2-ES), we computed pH values using output of 3-D DIC, alkalinity, temperature, and salinity and the OCMIP-2 carbon chemistry routines (Orr et al., 2000).

To be able to compute model-means and inter-model standard deviations, all variables were interpolated onto a common 1° × 1° regular grid and to standard ocean depths, using a Gaussian weighted average.

Preindustrial control simulations, for which atmospheric CO<sub>2</sub> and other greenhouse gases and aerosols are set to preindustrial levels, were used to remove potential century-scale model drifts. This correction is applied for all regional scale analysis and for global-average time-series of NPP, export production, O<sub>2</sub> and heat content. It is not applied for time series of surface pH and surface sea temperature for which no apparent long-term drift was detectable.

In the following analysis, we use both individual model results (for RCP8.5) and model-means (for all scenarios). In the case of model-means, no weighting functions are applied, i.e. all models contribute the same to the model mean.

Our core analysis is based on sea surface temperature, sea surface pH, vertically integrated NPP and O<sub>2</sub> averaged over 200–600 m. For O<sub>2</sub>, we focus first on this sub-surface depth interval to be able to describe changes in and around the oxygen minimum zones as well as changes in mid-latitude ventilated waters. Later, we complete

**BGD**

10, 3627–3676, 2013

### Multiple stressors of ocean ecosystems in the 21st century

L. Bopp et al.

Title Page

Abstract

Introduction

Conclusions

References

Tables

Figures

◀

▶

◀

▶

Back

Close

Full Screen / Esc

Printer-friendly Version

Interactive Discussion



the core analysis by extending it to make use of the full 3-D distribution of temperature, pH and dissolved O<sub>2</sub>.

The inter-model difference or model spread is used as an estimate of uncertainty around the projections. To show model agreement on global-mean time-series, we use one inter-model standard deviation. To show model agreement at the regional scale, we use stippling on the maps based on a simple robustness (or agreement) measure. Similar to the approach used for surface temperature changes in Meehl et al. (2007), high robustness for sea surface temperature and for pH is defined when the model-mean simulated change exceeds the inter-model standard deviation (the robustness index, defined as the ratio between model-mean simulated change and inter-model standard deviation is then larger than 1). Similar to the approach used for precipitation changes in Meehl et al. (2007), high robustness for oxygen and NPP is defined when at least 80 % of models agree on the sign of the mean change (robustness index larger than 1). Note that the estimate of uncertainty based on model spread may be biased by an arbitrary distribution of CMIP5 model output for a specific variable and by similarities between models (e.g. IPSL-CM5A-LR and IPSL-CM5A-MR share the same components differ in atmospheric resolution, see Table 1).

### 2.3 Water mass analysis

We used a global framework to group together water masses of similar behavior. Four classes were defined: Tropical Water (TW) masses, Mode and Intermediate Water (MIW) masses, Deep Water (DW) masses and Bottom Water (BW) masses. For example, the class MIW aims at gathering mode and intermediate waters of all basins, which share common features but are not distributed in the same range of density (Hanawa and Talley, 2001). Limits between classes were defined using several criteria (salinity, stratification, meridional velocities) resulting in different density thresholds in the five different basins (North Atlantic, South Atlantic, North Pacific, South Pacific and Indian Ocean) and for the different models. These density thresholds were computed

**BGD**

10, 3627–3676, 2013

## Multiple stressors of ocean ecosystems in the 21st century

L. Bopp et al.

Title Page

Abstract

Introduction

Conclusions

References

Tables

Figures

◀

▶

◀

▶

Back

Close

Full Screen / Esc

Printer-friendly Version

Interactive Discussion



for each model using the first ten years (2006–2015) of scenario RCP4.5 (temperature, salinity etc.) and the density referenced to 2000 m ( $\sigma_2$ ).

The limit between well stratified TW and homogeneous MIW was defined using a stratification criteria ( $\partial\sigma_2/\partial z > 0.02 \text{ kg m}^{-4}$ , with  $z$  the depth). The lower boundary of MIW was defined as the depth where the salinity is equal to its deep minimum value +0.05. DW were distinguished from BW using the deepest change in sign of meridional velocities, orientated northward in BW and southward in DW. Note that in the North Atlantic MIW are not associated with a deep salinity minimum. Instead the limit between MIW and DW was defined as a minimum in meridional velocities, which are oriented southward in both water masses.

### 3 Results and discussion

A thorough evaluation, using data-based products, of all simulations used here is beyond the scope of this study. Most models, including their marine biogeochemical components, have been evaluated individually elsewhere (see references in Table 1).

Here, we briefly discuss global mean-values of present day SST, surface pH, oceanic  $\text{O}_2$  content and integrated NPP, as listed in Table 2 for each individual model. We also show a regional comparison to data-based products of present-day model-mean SST, surface pH, sub-surface  $\text{O}_2$  and NPP (Fig. 1). Finally the skill of the different models in representing spatial and temporal variability of data-based fields are quantified while relying on Taylor diagrams (Taylor, 2001, Fig. 2).

Whereas large-scale patterns are well represented for SST and sub-surface  $\text{O}_2$ , the comparison to data-based products is much less satisfying for surface pH and NPP (Fig. 1). This is also reflected in the Taylor diagrams, with correlation coefficient ( $R$ ) ranging from 0.98 to 1.0 for SST, from 0.7 to 0.95 for  $\text{O}_2$ , but from 0.1 to 0.6 for pH and from 0.2 to 0.6 for NPP (Fig. 2). For NPP, the models score poorly because we do not include the seasonal cycle in the correlation, and (2) they under-represent high productivity in coastal regions. Additionally models that do perform well for one variable

**BGD**

10, 3627–3676, 2013

## Multiple stressors of ocean ecosystems in the 21st century

L. Bopp et al.

Title Page

Abstract

Introduction

Conclusions

References

Tables

Figures

◀

▶

◀

▶

Back

Close

Full Screen / Esc

Printer-friendly Version

Interactive Discussion





---

**Multiple stressors of ocean ecosystems in the 21st century**L. Bopp et al.

---

[Title Page](#)[Abstract](#)[Introduction](#)[Conclusions](#)[References](#)[Tables](#)[Figures](#)[⏪](#)[⏩](#)[◀](#)[▶](#)[Back](#)[Close](#)[Full Screen / Esc](#)[Printer-friendly Version](#)[Interactive Discussion](#)

by the climate models. However, most of it arises from model differences in (1) climate sensitivities (Knutti and Hegerl, 2008) and to (2) the way RCP scenarios are set up, i.e. aerosols and some greenhouse gases concentrations other than CO<sub>2</sub> may differ between models for the same scenario (Szopa et al., 2012). For example, the SST warming for the RCP8.5 scenario reaches +3.5 °C in three of the models (MPI-ESM-LR, IPSL-CM5A-LR and IPSL-CM5A-MR) and only 2.25 °C in two others (GFDL-ESMs) (Fig. 4). This is explained by the differences in climate sensitivity: IPSL-CMs and MPI-ESM-LR have high 2×CO<sub>2</sub> equilibrium climate sensitivities, whereas the GFDL-ESMs are on the low range of climate sensitivities as demonstrated by Andrews et al. (2012b).

Sea surface pH decreases as a consequence of the ocean taking up a significant fraction of anthropogenic carbon accumulated in the atmosphere. Even more than for SST, the magnitude of pH decrease is entirely dictated by the scenario (for a given atmospheric CO<sub>2</sub> concentrations). In the 2090s, the drop in global-average surface pH compared to 1990s values amounts to −0.33 (±0.003), −0.22 (±0.002), −0.15 (±0.001) and −0.07 (±0.001) pH unit, for RCP8.5, RCP6.0, RCP4.5 and RCP2.6 respectively (Fig. 3, Table 3). The model-mean projection for RCP8.5 is similar to that by Orr et al. (2005) for the IS92a scenario. In this scenario, the surface pH decrease of 0.3–0.4 units by 2100 translates into a 100 to 150 % increase in H<sup>+</sup> concentration. Simultaneously, carbonate ion concentrations decrease everywhere and eventually reach aragonite undersaturation in the surface waters of the Southern Ocean and the North Pacific (Orr et al., 2005). Even earlier aragonite undersaturation could be reached in the Arctic waters as demonstrated by Steinacher et al. (2009).

In contrast to SST projections, the model spread for global surface pH projections (estimated as the inter-model standard deviation) is very low (less than 0.003 pH unit). This is explained by: (1) the weak interannual variability in global mean surface pH (Fig. 4), (2) a weak climate-pH feedbacks, as demonstrated in Orr et al. (2005) for earlier Earth System Models, (3) the similar carbonate chemistry equations and well-defined constants based on the OCMIP-2 protocol used by most, if not all, models (Orr et al., 2000) and (4) the uniqueness of the ocean acidification forcing, i.e. of



## Multiple stressors of ocean ecosystems in the 21st century

L. Bopp et al.

Title Page

Abstract

Introduction

Conclusions

References

Tables

Figures



Back

Close

Full Screen / Esc

Printer-friendly Version

Interactive Discussion



a decline in integrated NPP, ranging from  $-2\%$  to  $-13\%$ , from 1860 to 2100 under the SRES A2 scenario (Steinacher et al., 2010). Those simulated decreases were primarily attributed to reduced nutrient supply to the surface in the tropics and temperate ocean due to enhanced stratification and reduced ocean ventilation. However other modeling studies find that integrated NPP increases during in the 21st century, even though simulated new production and export production still decrease (Schmittner et al., 2008; Taucher and Oschlies, 2011). The decoupling between export production and net primary production in these latter studies has been shown to be driven by the direct effects of temperature on biological processes such as remineralization rates. These links are explored further in Sect. 3.2.3.

The large inter-model spread in NPP is obvious on Fig. 3 for all scenarios and illustrated for RCP8.5 on Fig. 4. While this large spread is partly linked to the large interannual variability of NPP, as simulated by some models (e.g. HadGEM2-ES, NorESM1-ME and MPI-ESMs), it is mainly due to large model differences. Some models (GFDL-ESMs) simulate a slight decrease of globally integrated NPP (between 0 and  $-2\%$  in 2100), whereas others (MPI-ESMs, and HadGEM2-ES) simulate a large decrease (between  $-12$  and  $-18\%$  in 2100). The fact that models of the same family (IPSL-CM5A-LR and IPSL-CM5A-MR, MPI-ESM-LR and MPI-ESM-MR, GFDL-ESM2G and GFDL-ESM2M, respectively), which share the same biogeochemical component, project similar changes in globally-integrated NPP (Fig. 4) suggests that differences in marine biogeochemical model parameterizations explain model differences, at least from a global perspective.

## 3.2 Regional contrasts in multi-stressor projections

### 3.2.1 General description

Unlike global mean projections, simulated changes in temperature, pH,  $O_2$  and NPP have contrasting regional patterns. Figures 5 and 6 show the changes of SST, surface pH, averaged  $O_2$  concentrations over 200–600 m and vertically integrated NPP,

between 1990s and 2090s, and for the two extreme scenarios, RCP8.5 and RCP2.6 respectively. Local model agreement, based on a robustness index detailed in Sect. 2.2, is indicated by stippling.

Changes in SST are not spatially uniform. Stronger warming occurs in the tropics, in the North Pacific and in the Arctic Ocean, with SST increases larger than 4 °C in the RCP8.5 scenario (Fig. 5). On the contrary, much weaker warming, even cooling, is simulated in the North Atlantic and in some parts of the Southern Ocean, where deep convection is strongly reduced or where sea-ice remains unchanged. Robustness of these regional projections is high (Knutti and Sedlacek, 2012), even for the low-emission scenario RCP2.6 (Fig. 6). Only the regions with a weak signal show low robustness, which is a consequence of the signal-to-noise metric used here to estimate robustness (the ratio of model-mean change over inter-model standard deviation).

Changes in surface pH are smoother and more uniform than SST changes, and very robust across models. Surface pH changes range from -0.25 to -0.45 pH unit in RCP8.5 and from -0.05 to -0.15 RCP2.6 (Figs. 5 and 6). Larger changes occur in the surface Arctic Ocean for both scenarios. This is consistent with recent results obtained with the MIROC ESM under the RCP8.5 scenario (Yamamoto et al., 2012). The authors showed that Arctic sea-ice melting amplifies the decrease of surface pH due to the uptake of anthropogenic carbon, consistent with Steinacher et al. (2009).

Changes in sub-surface (200–600 m) O<sub>2</sub> are not spatially uniform and there is less agreement among models. But despite a strong difference in magnitude, the complex patterns of spatial changes are very similar across the two scenarios and reflect the influence of changes in several processes (ventilation, vertical mixing, remineralization) on O<sub>2</sub> levels (Figs. 5 and 6). The North Pacific, the North Atlantic, the Southern Ocean, the subtropical South Pacific and South Indian Oceans all undergo deoxygenation, with O<sub>2</sub> decreases of as much as -50 mmol m<sup>-3</sup> in the North Pacific for the RCP8.5 scenario. In contrast, the tropical Atlantic and the tropical Indian show increasing O<sub>2</sub> concentrations in response to climate change, in both RCP8.5 and RCP2.6 scenarios. The equatorial Pacific displays a weak east-west dipole, with increasing O<sub>2</sub> in the east

## BGD

10, 3627–3676, 2013

### Multiple stressors of ocean ecosystems in the 21st century

L. Bopp et al.

Title Page

Abstract

Introduction

Conclusions

References

Tables

Figures



Back

Close

Full Screen / Esc

Printer-friendly Version

Interactive Discussion



and decreasing O<sub>2</sub> in the west. Apart from changes in the equatorial Pacific, these regional changes in sub-surface O<sub>2</sub> are consistent across models under the RCP8.5 scenario (stippling on Fig. 5), and they are quite similar to those from a recent inter-model comparison of the previous generation of earth system models (Cocco et al., 2012).

Over the mid-latitudes, patterns of projected changes in sub-surface O<sub>2</sub> are broadly consistent with observations collected over the past several decades (Helm et al., 2011; Stendardo and Gruber, 2012; Takatani et al., 2012). Yet there is no such model-data agreement over most of the tropical oceans. Observed time series suggest a vertical expansion of the low-oxygen zones in the eastern tropical Atlantic and the equatorial Pacific during the past 50 yr (Stramma et al., 2008), conversely with models that simulate increasing O<sub>2</sub> levels with global warming over the historical period (Andrews et al., 2012a). A more detailed analysis of the simulated evolution of volumes of low-oxygen waters is given in Sect. 3.2.4.

Similar to sub-surface O<sub>2</sub> and in line with previous modeling studies (Bopp et al., 2001; Steinacher et al., 2010), projected changes in NPP are spatially heterogeneous. A decrease in NPP is consistently simulated across models and scenarios in the tropical Indian Ocean, in the west tropical Pacific, in the tropical Atlantic and in the North Atlantic (Figs. 5 and 6). This decrease reaches as much as  $-150 \text{ g C m}^{-2} \text{ yr}^{-1}$  regionally in 2090s for the RCP8.5 scenario, more than a 50 % decrease in historical levels of NPP in the North Atlantic, while at the same time there is a 30 % decrease in the tropical Indian and west tropical Pacific. In the eastern equatorial Pacific, the model-mean also indicates a large decrease of NPP, but this response is not consistent across models, with 3 models (GFDL-ESMs and CESM1-BGC) simulating an increase in NPP in response to climate change in that region (eastern Equatorial Pacific). The main mechanisms responsible for NPP decreases in the tropics and in the North Atlantic have been identified in a previous model inter-comparison study (Steinacher et al., 2010) and are linked to a reduced supply of nutrients to the euphotic zone in response to enhanced stratification and slowed circulation.

## BGD

10, 3627–3676, 2013

### Multiple stressors of ocean ecosystems in the 21st century

L. Bopp et al.

Title Page

Abstract

Introduction

Conclusions

References

Tables

Figures



Back

Close

Full Screen / Esc

Printer-friendly Version

Interactive Discussion



Finally, the mean of the CMIP5 models exhibits increased NPP in the western North Pacific, the Arctic Ocean, and in parts of the Southern Ocean (Figs. 5 and 6). These changes are consistent across models for the RC8.5 scenario but not for the RCP2.6 scenario. Mechanisms that could explain such an increase in NPP are related to an alleviation of light- and/or temperature limitation as shown by Steinacher et al. (2010), and to increased nutrient supply in upwelling regions under a shoaling nutricline (Rykaczewski and Dunne, 2010).

We now turn to three specific questions related to the changes of pH at depth, the links between projected changes of NPP and export production, and the evolution of oxygen minimum zones.

### 3.2.2 Projected pH changes over depth

Direct observations of pH from available time-series show consistent trends of decreasing pH of about 0.02 pH unit per decade for the surface ocean (Bindoff et al., 2007). However, several recent studies have reported more rapid reductions of pH at sub-surface (between 200 and 300 m) in the sub-tropical oceans (Bates et al., 2012; Dore et al., 2009; Ishii et al., 2011), which can be explained solely by a lower carbonate buffering capacity of these sub-surface waters (Orr, 2011).

These larger subsurface changes in pH could occur at depth relative to the surface, are consistent across all models used here. In 2090s and for the RCP8.5 scenario, maximum pH changes are located at the surface in the high latitude oceans and in upwelling regions, but at 100 to 400 m depth in the sub-tropics (Fig. 7). These changes of sub-surface pH are 0.05 pH unit larger than the comparable surface changes (Fig. 7). The build-up of this sub-surface low-pH water may have implications on the timing of pH changes at the surface when these water-masses are brought/mixed back to the surface (Resplandy et al., 2013).

**BGD**

10, 3627–3676, 2013

## Multiple stressors of ocean ecosystems in the 21st century

L. Bopp et al.

Title Page

Abstract

Introduction

Conclusions

References

Tables

Figures

◀

▶

◀

▶

Back

Close

Full Screen / Esc

Printer-friendly Version

Interactive Discussion



### 3.2.3 Projected changes of NPP and export production

Model-mean projections of changes in export production are shown for RCP8.5 in Fig. 8. These changes display very similar patterns to those of NPP (Fig. 5), with increasing export production in the Arctic Ocean and in parts of the Southern Ocean, and decreasing export production in the tropical oceans, and in the North Atlantic. Interestingly, robustness of the model-mean projection is larger for export production than for NPP projections: 38 % of  $1^\circ \times 1^\circ$  ocean pixels have a robustness index of more than 1 for projected NPP whereas 45 % of the same pixels have a robustness index greater than 1 for projected export production. This is especially the case for the eastern equatorial Pacific, where 8 out of 9 models project a decrease of export production with climate change, whereas the response for NPP is split between an increase (3 models) and a decrease (6 models). For instance, GFDL-ESM2G and GFDL-ESM2M simulate a decoupling of export and primary production in that region, i.e. decreased export production and increased NPP.

For the global-average, this increased model consistency for simulated changes in export production versus those for NPP is also apparent (Fig. 8). For the RCP8.5 scenario, projected changes in the 2090s for export production reach  $-7$  to  $-18$  % (inter-model standard deviation is 5.9%), whereas for NPP they range between  $-2$  and  $-16$  % (inter-model standard deviation is 7.9%).

Taucher and Oschlies (2011) have explored the parallel responses of NPP and export production to climate change using a simple NPZD model in which they vary the dependence of production and remineralization rates to temperature. They show that when rates that are highly dependent on temperature are taken into account, elevated temperatures lead to enhanced NPP and accelerated carbon recycling, which is opposite to what is shown here with the CMIP5 models. However, whether or not temperature-dependent rates are used, simulated export production decreases with climate change in their simulations, as with previous model studies (Bopp et al., 2001). Note that the almost all of the biogeochemical components of the CMIP5 models

BGD

10, 3627–3676, 2013

## Multiple stressors of ocean ecosystems in the 21st century

L. Bopp et al.

Title Page

Abstract

Introduction

Conclusions

References

Tables

Figures



Back

Close

Full Screen / Esc

Printer-friendly Version

Interactive Discussion



include temperature-dependent production and remineralization rates, but it is likely that they also use very different parameter values, which would explain the large discrepancy in NPP projections.

Whereas global export production seems to be mostly controlled by the balance between reduction in nutrients supplied to the euphotic layer and alleviation of light and temperature limitations (but also by changes in plankton community as shown by Bopp et al., 2005), larger uncertainties in projections of NPP emphasize the need to improve model representations of more direct biological effects, such as the temperature-dependency of physiological rates studied by Taucher and Oschlies (2011).

### 3.2.4 Projected changes in the extension of Oxygen Minimum Zones

Oxygen Minimum Zones (OMZs) are key oceanic regions because of their role in the marine nitrogen cycle (water-column denitrification occurs almost exclusively in O<sub>2</sub>-deficient waters) and because of the unusual ecosystems associated with low-O<sub>2</sub> regions (OMZs represent a respiratory barrier for many organisms).

Following Cocco et al. (2012), we used three different thresholds (5, 50 and 80 mmol m<sup>-3</sup>) to characterize water volumes of low-oxygen waters. Suboxic waters are defined with a threshold of 5 mmol m<sup>-3</sup> whereas hypoxic waters are defined here with a threshold of 50 mmol m<sup>-3</sup>. Figure 9 presents the relative evolution of these 3 volumes as simulated by the CMIP5 models over 1870 to 2100 and for the RCP8.5 scenario. Although each model is plotted for each of the three volumes on Fig. 9, we highlight the models for which the simulated volumes over 1990–1999 fall within +100 % and –50 % of the observed volumes (126, 60 and 2.6 millions of km<sup>3</sup> respectively), as estimated from the revised WOA2005 database (Bianchi et al., 2012).

By 2100, all models project an increase in the volume of waters below 80 mmol m<sup>-3</sup>, ranging from +1 % (MPI-ESMs) to +9 % (CESM1-BGC), relative to 1990–1999. This response is more consistent than that of the previous generation of earth system models, i.e. changes varying from –26 to +16 % over 1870 to 2099 under the SRES-A2 scenario (Cocco et al., 2012). Conversely, for lower oxygen levels, there is less

BGD

10, 3627–3676, 2013

## Multiple stressors of ocean ecosystems in the 21st century

L. Bopp et al.

Title Page

Abstract

Introduction

Conclusions

References

Tables

Figures

◀

▶

◀

▶

Back

Close

Full Screen / Esc

Printer-friendly Version

Interactive Discussion



## Multiple stressors of ocean ecosystems in the 21st century

L. Bopp et al.

Title Page

Abstract

Introduction

Conclusions

References

Tables

Figures



Back

Close

Full Screen / Esc

Printer-friendly Version

Interactive Discussion



agreement among the CMIP5 models. Simulated volumes do not agree with observations, and changes due to climate change may be either negative or positive. For the volume of waters below  $50 \text{ mmol m}^{-3}$ , four models project an expansion of 2 % to 16 % (both GFDL-ESMs, HadGEM2-ES and CESM1-BGC), whereas two other models project a slight contraction of  $\sim 2\%$  (NorESM1-ME and MPI-ESM-MR). For the volume of waters below  $5 \text{ mmol m}^{-3}$ , only one model (IPSL-CM5A-MR) is close to the volume estimated from observations and simulates a large expansion of this volume (+30 % in 2090s). These results for low- $\text{O}_2$  waters ( $5$  and  $50 \text{ mmol m}^{-3}$ ) agree with those of Cocco et al. (2012), with large model-data and model-model discrepancies and simulated responses varying in sign for the evolution of these volumes under climate change.

The ability of climate models to represent  $\text{O}_2$  observations has been questioned in recent studies. Stramma et al. (2012) used an ESM of intermediate complexity to perform simulations over the historical period and compared the simulated sub-surface  $\text{O}_2$  trends with observations. They showed that the model was unable to reproduce the spatial patterns of observed changes. Similarly, Andrews et al. (2012a) compared output of MPI-ESM-LR and HadGEM2-ES to observations over the historical period. They reported that both models fail to reproduce the pattern of  $\text{O}_2$  loss recorded by observations in low-latitude OMZs.

A more thorough analysis of the mechanisms responsible for the model-data discrepancies as well as the mechanisms driving the simulated future changes is necessary. Gnanadesikan et al. (2012) performed such an analysis with simulations carried out with a previous version of the GFDL Earth System Model (GFDL-ESM2.1) under the SRES-A2 scenario. They show that the volume of suboxic waters does not increase under global warming in the tropical Pacific. A detailed analysis of the different terms contributing to the  $\text{O}_2$  budget showed that an increase in  $\text{O}_2$  in very low oxygen waters is associated to an enhanced supply of  $\text{O}_2$  through lateral diffusion and increased ventilation along the Chilean coast. These results cast doubt on the ability of the present generation of models to project changes in  $\text{O}_2$  accurately at the regional level, especially for low- $\text{O}_2$  waters, and stress the need for more model-data

comparison over the historical period alongside a better understanding of reasons for model biases.

### 3.3 Relation between stressors and across scenarios

#### 3.3.1 Global scale

5 The existence of potential synergistic effects between the different stressors discussed here emphasizes the need to study them together (Boyd et al., 2008). Figure 10 shows the temporal model-mean evolution of global surface pH, global oxygen content and global NPP versus global sea surface warming for each of the RCPs over 2006–2099. For RCP8.5, all these relationships appear linear, implying a constant fraction of acidification, deoxygenation, and NPP reduction per degree of warming: mean surface pH decreases by 0.127 pH unit  $^{\circ}\text{C}^{-1}$ , global oxygen content decreases by 1.3 %  $^{\circ}\text{C}^{-1}$  and global NPP loses 3.3 %  $^{\circ}\text{C}^{-1}$  (with  $R^2$  of 0.99, 0.99 and 0.95 respectively).

For the other RCPs scenarios, relationships are similar for surface pH vs. SST and for NPP vs. SST, but the relationship breaks down for oxygen content versus sea surface warming (Fig. 10). That is, deoxygenation continues long after sea surface temperatures have stabilized. In particular for the RCP2.6 scenario, the total content of oxygen in the ocean loses an additional 1 % in the second half of the 21st century after sea surface warming has been stabilized at  $+0.7^{\circ}\text{C}$  in 2050 (Fig. 3). When plotted against heat content change however, a single linear relationship for  $\text{O}_2$  content emerges across the different scenarios with a slope of  $\sim -0.149\%/10^{22}\text{ J}$  or  $3.9\text{ nmolJ}^{-1}$  ( $R^2 > 0.99$ ) in the RCP8.5 scenario (Fig. 10). This slope of  $3.9\text{ nmol O}_2\text{J}^{-1}$  is slightly lower than that found in early deoxygenation studies (e.g.  $6\text{ nmolJ}^{-1}$  in Bopp et al., 2002), but more consistent with the recent study of Frölicher et al. (2009), thus indicating a larger contribution (here around 40 %) of warming-induced solubility reduction in global deoxygenation (which contribution is estimated at  $1.5\text{ nmolJ}^{-1}$ , Bopp et al., 2002).

BGD

10, 3627–3676, 2013

## Multiple stressors of ocean ecosystems in the 21st century

L. Bopp et al.

Title Page

Abstract

Introduction

Conclusions

References

Tables

Figures

◀

▶

◀

▶

Back

Close

Full Screen / Esc

Printer-friendly Version

Interactive Discussion



### 3.3.2 Analysis within a water-mass framework

For more insight into regional relationships between the different stressors, we computed trends of temperature, pH and O<sub>2</sub> in distinct water-masses as described in the methodology section. Because coupled climate models have strong biases in the way they simulate the distribution of the main oceanic water masses (see Saltee et al., 2012 for an evaluation of Southern Ocean water masses in the CMIP5 models), this water mass framework is a natural approach to analyze model behavior (Iudicone et al., 2011) or to compare models. Furthermore, it avoids averaging biogeochemical properties between different water masses.

Figure 11 details the global relationships between temperature and pH and between temperature and O<sub>2</sub>, respectively, across the different RCP scenarios and for the four distinct water masses (WM).

Not surprisingly, this analysis reveals large differences between the different WM, and for instance between tropical waters (TW) and mode/intermediate waters (MIW). TW are characterized by relatively low acidification-to-warming and low deoxygenation-to-warming ratios (Fig. 11). In contrast, MIW are characterized by much higher acidification- and deoxygenation-to-warming ratios, demonstrating the importance of these water masses in the propagation of the acidification and deoxygenation signals to the ocean's interior. In addition, MIW have a low buffer capacity of the carbonate system thus amplifying the response of pH to the uptake of anthropogenic carbon (see Sect. 3.2.2). The deep and bottom water masses (DW and BW) show very little acidification and warming trends, but some significant deoxygenation trend for the high-emission scenarios (RCP8.5).

The climate change patterns differ when the model results are distinguished by oceanic basin. Figure 12 shows the relationships between pH and temperature, and between O<sub>2</sub> and temperature for 3 of the 4 WMs (omitting TW), averaged over large oceanic basins (North Atlantic, North Pacific and Southern Ocean) for RCP8.5 (2090s minus 2000s). Remarkably, the responses of different stressors in the water masses

BGD

10, 3627–3676, 2013

## Multiple stressors of ocean ecosystems in the 21st century

L. Bopp et al.

Title Page

Abstract

Introduction

Conclusions

References

Tables

Figures



Back

Close

Full Screen / Esc

Printer-friendly Version

Interactive Discussion



## Multiple stressors of ocean ecosystems in the 21st century

L. Bopp et al.

Title Page

Abstract

Introduction

Conclusions

References

Tables

Figures



Back

Close

Full Screen / Esc

Printer-friendly Version

Interactive Discussion



of different basins are distinct and relatively robust across the range of models used here, demonstrating the promise of such an approach. The North Pacific and the Southern Ocean display similar behavior with similar ratios of acidification-to-warming and deoxygenation-to-warming for the different water masses with larger changes in both stressors for MIW and less in deep and bottom waters. The Southern Ocean shows, however, stronger signals than the North Pacific for MIW and BW, whereas the North Pacific shows stronger signals for DW (Fig. 12). WM of the North Atlantic are characterized by much larger uncertainties (model spread) and by acidification and deoxygenation-to-warming ratios different from the ratios of other basins (Fig. 12). The North Atlantic MIW shows very small changes in temperature and oxygen, but a large and robust signal in pH ( $-0.26$  pH unit). In the North Atlantic DW, the models project a very strong acidification and deoxygenation signals, with  $-0.16$  pH unit and  $-13$   $\text{mmol m}^{-3}$  for a warming of only  $0.1$ – $0.2$   $^{\circ}\text{C}$ .

Although a more thorough analysis is needed to assess the mechanisms responsible for these changes and their relationship with ocean circulation and water mass formation, this first analysis illustrates the unique character of MIW, across the ocean, in terms of its intensity of deoxygenation and acidification. This study also reveals strong differences between the North Atlantic relative to the Southern Ocean and the North Pacific. The large model spread for warming and deoxygenation in the North Atlantic, for all water masses, is linked to large differences between models for the weakening of the Atlantic Meridional Overturning Circulation (Cheng et al., 2013) and for changes in the distribution of North Atlantic WM.

## 4 Conclusions

Using here 10 ESMs participating to the recent Coupled Model Intercomparison Project 5, we assess how the major stressors of marine ecosystems, namely ocean temperature, pH, dissolved oxygen concentrations and primary productivity may evolve over the course of the 21st century and under several atmospheric  $\text{CO}_2$  pathways. All models

**BGD**

10, 3627–3676, 2013

**Multiple stressors of ocean ecosystems in the 21st century**

L. Bopp et al.

[Title Page](#)[Abstract](#)[Introduction](#)[Conclusions](#)[References](#)[Tables](#)[Figures](#)[Back](#)[Close](#)[Full Screen / Esc](#)[Printer-friendly Version](#)[Interactive Discussion](#)

project consistent warming, acidification, deoxygenation and lowering of primary productivity, whose intensities strongly depend on the scenario. Sea surface warming, sea surface pH reduction, decrease in global oxygen content and decrease in integrated primary productivity range from +0.71 to +2.73 °C, from –0.07 to –0.33 pH unit, from –1.81 to –3.45 %, and from –2.0 to –8.6 %, respectively, in 2090s compared to 1990s and for all RCPs scenarios covered here.

Turning to the regional scale, the simulated evolution of the different stressors differ (Figs. 5 and 6). Figure 13 summarizes the regional responses of the different stressors at the end of the 21st century under RCP8.5 scenario. In brief, the tropical oceans are characterized by high warming rates, low acidification rates, inconsistent changes in sub-surface oxygen, and high rates of NPP decrease. The North Pacific is characterized by high warming rates, high acidification rates, large decrease in sub-surface oxygen and a mixed and inconsistent response in NPP. The North Atlantic is characterized by low warming rates, high acidification rates, medium-to-large decrease of sub-surface oxygen and large decrease of NPP. Finally, the Southern Ocean is characterized by very low warming rates, high acidification rates, medium-to-large decrease of sub-surface oxygen and a mixed response in NPP.

The mechanisms explaining these modifications are not analyzed in detail here, but consistency with previous model intercomparison studies suggest continued robustness in the general drivers of these changes. Ocean acidification is driven by the atmospheric evolution of CO<sub>2</sub> with little feedback from climate change. Regional modulations of acidification rates are explained by differences in uptake rates of anthropogenic carbon and in carbonate buffering capacities of the different water masses. Deoxygenation is due to a warming-induced reduction in solubility, but also to increased stratification and reduced ventilation. Reduction of NPP in the tropics and in the North Atlantic is also due to increased stratification and reduced ventilation, but increasing NPP at higher latitudes is explained by an alleviation of light- and/or temperature limitation. Lack of robustness for these projections is especially critical for low latitude sub-surface

O<sub>2</sub>-concentrations (and OMZs evolution) and for NPP in some high-productivity regions such as the east Equatorial Pacific.

One critical improvement in future ESMs will be amelioration of biases in the representation of OMZs. A related long term goal will be vastly-enhanced resolution to represent the scales of coastal upwelling and other mesoscale phenomena such as eddies. Finally, representation of ecosystems in models such as these is an evolving science. They represent only a small set of the processes controlling ecosystem and biogeochemical function. While the models are each constructed in mathematically-defensible forms, they are all different in the underlying assumptions. Rather than representing discrete biological forms, they represent ecosystems as a biological continuum with infinite biodiversity in some ways (i.e. the role of temperature), and an artificial rigidity in others (i.e. fixed half saturation constants).

*Acknowledgements.* We acknowledge the World Climate Research Programme's Working Group on Coupled Modelling, which is responsible for CMIP. For CMIP the US Department of Energy's Program for Climate Model Diagnosis and Intercomparison provides coordinating support and led development of software infrastructure in partnership with the Global Organization for Earth System Science Portals. The authors also thank the IPSL modeling group for the software infrastructure that facilitates CMIP5 analysis. This work was supported through EU FP7 project CARBOCHANGE, EU FP7 project MEECE, and ANR project MACROES. S.C.D. acknowledges the US National Science Foundation (AGS-1048827)..



The publication of this article is financed by CNRS-INSU.

## Multiple stressors of ocean ecosystems in the 21st century

L. Bopp et al.

Title Page

Abstract

Introduction

Conclusions

References

Tables

Figures



Back

Close

Full Screen / Esc

Printer-friendly Version

Interactive Discussion



## References

- Andrews, O. D., Bindoff, N. L., Halloran, P. R., Ilyina, T., and Le Quéré, C.: Detecting an external influence on recent changes in oceanic oxygen using an optimal fingerprinting method, *Biogeosciences Discuss.*, 9, 12469–12504, doi:10.5194/bgd-9-12469-2012, 2012a.
- 5 Andrews, T., Gregory, J. M., Webb, M. J., and Taylor, K. E.: Forcing, feedbacks and climate sensitivity in CMIP5 coupled atmosphere-ocean climate models, *Geophys. Res. Lett.*, 39, L09712, doi:10.1029/2012GL051607, 2012b.
- Assmann, K. M., Bentsen, M., Segschneider, J., and Heinze, C.: An isopycnic ocean carbon cycle model, *Geosci. Model Dev.*, 3, 143-167, doi:10.5194/gmd-3-143-2010, 2010.
- 10 Aumont, O. and Bopp, L.: Globalizing results from ocean in situ iron fertilization studies, *Global Biogeochem. Cy.*, 20, 1–15, 2006.
- Bates, N. R., Best, M. H. P., Neely, K., Garley, R., Dickson, A. G., and Johnson, R. J.: Detecting anthropogenic carbon dioxide uptake and ocean acidification in the North Atlantic Ocean, *Biogeosciences*, 9, 2509–2522, doi:10.5194/bg-9-2509-2012, 2012.
- 15 Behrenfeld, M. J. and Falkowski, P. G.: Photosynthetic rates derived from satellite-based chlorophyll concentration, *Limnol. Oceanogr.*, 42, 1, 1–20, 1997.
- Behrenfeld, M. J., O'Malley, R. T., Siegel, D. A., McClain, C. R., Sarmiento, J. L., Feldman, G. C., Milligan, A. J., Falkowski, P. G., Letelier, R. M., and Boss, E. S.: Climate-driven trends in contemporary ocean productivity, *Nature*, 444, 752–755, 2006.
- 20 Bentsen, M., Bethke, I., Debernard, J. B., Iversen, T., Kirkevåg, A., Seland, Ø., Drange, H., Roe-landt, C., Seierstad, I. A., Hoose, C., and Kristjánsson, J. E.: The Norwegian Earth System Model, NorESM1-M – Part 1: Description and basic evaluation, *Geosci. Model Dev. Discuss.*, 5, 2843–2931, doi:10.5194/gmdd-5-2843-2012, 2012.
- Bianchi, D., Dunne, J., Sarmiento, J., and Galbraith, E.: Data-based estimates of suboxia, denitrification and N<sub>2</sub>O production in the ocean, and their sensitivities to change, *Global Biogeochem. Cy.*, 26, 6550–6555, 2012.
- 25 Bindoff, N., Willebrand, J., Artale, V., Cazenave, A., Gregory, J., Gulev, S., Hanawa, K., Le Quere, C., Levitus, S., Norjiri, Y., Shum, C., Talley, L., and Unnikrishnan, A.: Observations: oceanic climate change and sea level, in: *Climate Change 2007: The Physical Science Basis, Contribution of Working Group I to the Fourth Assessment Report of the Intergovernmental Panel on Climate Change*, edited by: Solomon, S., Qin, D., Manning, M., Chen, Z., Marquis, M., Averyt, K. B., Tignor, M., and Miller, H. L., Tech. Rep., Intergovernmental Panel
- 30

## Multiple stressors of ocean ecosystems in the 21st century

L. Bopp et al.

Title Page

Abstract

Introduction

Conclusions

References

Tables

Figures



Back

Close

Full Screen / Esc

Printer-friendly Version

Interactive Discussion



on Climate Change, Cambridge University Press, Cambridge, UK and New York, NY, USA, 2007.

Bopp, L., Monfray, P., Aumont, O., Dufresne, J. L., Le Treut, H., Madec, G., Terray, L., and Orr, J. C.: Potential impact of climate change on marine export production, *Global Biogeochem. Cy.*, 15, 81–99, 2001.

Bopp, L., Le Quéré, C., Heimann, M., Manning, A. C., and Monfray, P.: Climate-induced oceanic oxygen fluxes: implications for the contemporary carbon budget, *Global Biogeochem. Cy.*, 16, 1022, doi:10.1029/2001GB001445, 2002.

Boyce, D. G., Lewis, M. R., Worm, B.: Global phytoplankton decline over the past century, *Nature*, 466, 591–96, 2010.

Boyd, P. W., Doney, S. C., Strzepek, R., Dusenberry, J., Lindsay, K., and Fung, I.: Climate-mediated changes to mixed-layer properties in the Southern Ocean: assessing the phytoplankton response, *Biogeosciences*, 5, 847–864, doi:10.5194/bg-5-847-2008, 2008.

Cagnazzo, C., Manzini, E., Fogli, P. G., Vichi, M., and Davini, P.: Role of stratospheric dynamics in the ozone-carbon connection in the Southern Hemisphere, *Clim. Dynam.*, submitted, 2013.

Cocco, V., Joos, F., Steinacher, M., Frölicher, T. L., Bopp, L., Dunne, J., Gehlen, M., Heinze, C., Orr, J., Oschlies, A., Schneider, B., Segschneider, J., and Tjiputra, J.: Oxygen and indicators of stress for marine life in multi-model global warming projections, *Biogeosciences Discuss.*, 9, 10785–10845, doi:10.5194/bgd-9-10785-2012, 2012.

Doney, S. C.: The growing human footprint on coastal and open-ocean biogeochemistry, *Science*, 328, 1512–1516, 2010.

Doney, S. C., Lima, I., Moore, J. K., Lindsay, K., Behrenfeld, M. J., Westberry, T. K., Mahowald, N., Glover, D. M., and Takahashi, T.: Skill metrics for confronting global upper ocean ecosystem-biogeochemistry models against field and remote sensing data, *J. Marine Syst.*, 76, 95–112, 2009.

Doney, S. C., Ruckelshaus, M., Duffy, J. E., Barry, J. P., Chan, F., English, C. A., Galindo, H. M., Grebmeier, J. M., Hollowed, A. B., Knowlton, N., Polovina, J., Rabalais, N. N., Sydeman, W. J., and Talley, L. D.: Climate change impacts on marine ecosystems, *Annu. Rev. Mar. Sci.*, 4, 11–37, 2012.

Dore, J. E., Lukas, R., Sadler, D. W., Church, M. J., and Karl, D. M.: Physical and biogeochemical modulation of ocean acidification in the central North Pacific, *P. Natl. Acad. Sci. USA*, 106, 12235–12240, 2009.

**BGD**

10, 3627–3676, 2013

**Multiple stressors of ocean ecosystems in the 21st century**

L. Bopp et al.

Title Page

Abstract

Introduction

Conclusions

References

Tables

Figures

◀

▶

◀

▶

Back

Close

Full Screen / Esc

Printer-friendly Version

Interactive Discussion



## Multiple stressors of ocean ecosystems in the 21st century

L. Bopp et al.

Title Page

Abstract

Introduction

Conclusions

References

Tables

Figures

◀

▶

◀

▶

Back

Close

Full Screen / Esc

Printer-friendly Version

Interactive Discussion

- Dufresne, J.-L., Foujols, M.-A., Denvil, S., Caubel, A., Marti, O., Aumont, O., Balkanski, Y., Bekki, S., Bellenger, H., Benschila, R., Bony, S., Bopp, L., Braconnot, P., Brockmann, P., Cadule, P., Cheruy, F., Codron, F., Cozic, A., Cugnet, D., de Noblet, N., Duvel, J.-P., Ethé, C., Fairhead, L., Fichefet, T., Flavoni, S., Friedlingstein, P., Grandpeix, J.-Y., Guez, L., Guilyardi, E., Hauglustaine, D., Hourdin, F., Idelkadi, A., Ghattas, J., Joussaume, S., Kageyama, M., Krinner, G., Labetoulle, S., Lahellec, A., Lefebvre, M.-P., Lefevre, F., Levy, C., Li, Z. X., Lloyd, J., Lott, F., Madec, G., Mancip, M., Marchand, M., Masson, S., Meurdesoif, Y., Mignot, J., Musat, I., Parouty, S., Polcher, J., Rio, C., Schulz, M., Swingedouw, D., Szopa, S., Talandier, C., Terray, P., and Viovy, N.: Climate change projections using the IPSL-CM5 Earth System Model: from CMIP3 to CMIP5, *Clim Dynam.*, accepted, 2013.
- Dunne, J. P., John, J., Adcroft, A., Griffies, S. M., Hallberg, R. W., Shevliakova, E., Stouffer, R. J., Cooke, W. F., Dunne, K. A., Harrison, M. J., Krasting, J. P., Malyshev, S., Milly, P. C. D., Phillipps, P., Sentman, L. T., Samuels, B. L., Spelman, M. J., Winton, M., Wittenberg, A. T., and Zadeh, N.: GFDL's ESM2 global coupled climate-carbon Earth System Models Part I: Physical formulation and baseline simulation characteristics, *J. Climate*, 25, 6646–6665, doi:10.1175/JCLI-D-11-00560.1, 2012a.
- Dunne, J. P., John, J. G., Shevliakova, E., Stouffer, R. J., Krasting, J. P., Malyshev, S., Milly, P. C. D., Sentman, L. T., Adcroft, A., Cooke, W. F., Dunne, K. A., Griffies, S. M., Hallberg, R. W., Harrison, M. J., Levy II, H., Wittenberg, A. T., Phillipps, P., and Zadeh, N.: GFDL's ESM2 global coupled climate-carbon Earth System Models Part II: Carbon system formulation and baseline simulation characteristics, *J. Climate*, doi:10.1175/JCLI-D-12-00150.1, 2012b.
- Friedlingstein P., Meinshausen, M., Arora, V. K., Jones, C. D., Liddicoat S. K., Knutti, R.: CMIP5 climate projections and uncertainties due to carbon cycle feedbacks, *J. Climate*, in review, 2013.
- Frölicher, T. L., Joos, F., Plattner, G. K., Steinacher, M., and Doney, S. C.: Natural variability and anthropogenic trends in oceanic oxygen in a coupled carbon cycle-climate model ensemble, *Global Biogeochem. Cy*, 23, GB1003, doi:10.1029/2008GB003316, 2009.
- Gent, P. R., Danabasoglu, G., Donner, L. J., Holland, M. M., Hunke, E. C., Jayne, S. R., Lawrence, D. M., Neale, R. B., Rasch, P. J., Vertenstein, M., Worley, P. H., Yang, Z.-L., and Zhang, M.: The community climate system model version 4, *J. Climate*, 24, 4973–4991, 2011.

## Multiple stressors of ocean ecosystems in the 21st century

L. Bopp et al.

[Title Page](#)

[Abstract](#)

[Introduction](#)

[Conclusions](#)

[References](#)

[Tables](#)

[Figures](#)

[◀](#)

[▶](#)

[◀](#)

[▶](#)

[Back](#)

[Close](#)

[Full Screen / Esc](#)

[Printer-friendly Version](#)

[Interactive Discussion](#)



Gilbert, D., Rabalais, N. N., Díaz, R. J., and Zhang, J.: Evidence for greater oxygen decline rates in the coastal ocean than in the open ocean, *Biogeosciences*, 7, 2283–2296, doi:10.5194/bg-7-2283-2010, 2010.

Giorgetta, M. A., Jungclaus, J. H., Reick, C. H., Legutke, S., Brovkin, V., Crueger, T., Esch, M., Fieg, K., Glushak, K., Gayler, V., Haak, H., Hollweg, H.-D., Ilyina, T., Kinne, S., Kornblueh, L., Matei, D., Mauritsen, T., Mikolajewicz, U., Mueller, W. A., Notz, D., Raddatz, T., Rast, S., Redler, R., Roeckner, E., Schmidt, H., Schnur, R., Segschneider, J., Six, K., Stockhause, M., Wegner, J., Widmann, H., Wieners, K.-H., Claussen, M., Marotzke, J., and Stevens, B.: Climate change from 1850 to 2100 in MPI-ESM simulations for the Coupled Model Intercomparison Project 5, submitted, 2013.

Gnanadesikan, A., Dunne, J. P., and John, J.: Understanding why the volume of suboxic waters does not increase over centuries of global warming in an Earth System Model, *Biogeosciences*, 9, 1159–1172, doi:10.5194/bg-9-1159-2012, 2012.

Gruber, N.: Warming up, turning sour, losing breath: ocean biogeochemistry under global change, *Philos. T. R. Soc. A*, 369, 1980–1996, 2011.

Hanawa, K. and Talley, L. D.: Mode waters, in: *Ocean Circulation and Climate*, edited by: Siedler, G. and Church, J., International Geophysics Series, Academic Press, 373–386, 2001.

Helm, K. P., Bindoff, N. L., and Church, J. A.: Observed decreases in oxygen content of the global ocean, *Geophys. Res. Lett.*, 38, L23602, doi:10.1029/2011GL049513, 2011.

Henson, S. A., Sarmiento, J. L., Dunne, J. P., Bopp, L., Lima, I., Doney, S. C., John, J., and Beaulieu, C.: Detection of anthropogenic climate change in satellite records of ocean chlorophyll and productivity, *Biogeosciences*, 7, 621–640, doi:10.5194/bg-7-621-2010, 2010.

Hofmann, G. E., Barry, J. P., Edmunds, P. J., Gates, R. D., Hutchins, D. A., Klinger, T., and Sewell, M. A.: The effects of ocean acidification on calcifying organisms in marine ecosystems: an organism to ecosystem perspective, *Annu. Rev. Ecol. Evol. S.*, 41, 127–47. 2010.

Hutchins, D. A., Fu, F.-X., Zhang, Y., Warner, M. E., Feng, Y., Portune, K., Bernhardt, P. W., and Mulholland, M. R.: CO<sub>2</sub> control of *Trichodesmium* N<sub>2</sub> fixation, photosynthesis, growth rates, and elemental ratios: Implications for past, present, and future ocean biogeochemistry, *Limnol. Oceanogr.*, 52, 1293–1304, 2007.

Ilyina, T., Six, K. D., Segschneider, J., Maier-Reimer, E., Li, H., and Nunez-Riboni, I.: The global ocean biogeochemistry model HAMOCC: Model architecture and performance as compo-

## Multiple stressors of ocean ecosystems in the 21st century

L. Bopp et al.

Title Page

Abstract

Introduction

Conclusions

References

Tables

Figures

◀

▶

◀

▶

Back

Close

Full Screen / Esc

Printer-friendly Version

Interactive Discussion



ment of the MPI-Earth System Model in different CMIP5 experimental realizations, submitted, 2013.

Ishii, M., Ishii, M., Inoue, H. Y., Midorikawa, T., Saito, S., Tokieda, T., Sasano, D., Nakadate, A., Nemoto, K., MetzI, N., Wong, C. S., and Feely, R. A.: Spatial variability and decadal trend of the oceanic CO<sub>2</sub> in the western equatorial Pacific warm/fresh water, *Deep-Sea Res. Pt. II*, 56, 591–606, 2009.

Iudicone, D., Rodgers, K. B., Stendardo, I., Aumont, O., Madec, G., Bopp, L., Mangoni, O., and Ribera d'Alcala', M.: Water masses as a unifying framework for understanding the Southern Ocean Carbon Cycle, *Biogeosciences*, 8, 1031–1052, doi:10.5194/bg-8-1031-2011, 2011.

Jones C. D., Robertson, E., Arora, V., Friedlingstein, P., Shevliakove, E., Bopp, L., Brovkin, V., Hajima, T., Kato, E., Kawamiya, M., Liddicoat, S., Lindsay, K., Reick, C., Roelandt, C., Segschneider, J., Tjiputra, J.: 21st Century compatible CO<sub>2</sub> emissions and airborne fraction simulated by CMIP5 Earth System models under 4 Representative Concentration Pathways, *J. Climate*, in press, 2013.

Keeling, R. F., Körtzinger, A., and Gruber, N.: Ocean deoxygenation in a warming world, *Annu. Rev. Mar. Sci.*, 2, 199–229, doi:10.1146/annurev.marine.010908.163855, 2010.

Knutti, R. and Hegerl, G. C.: The equilibrium sensitivity of the Earth's temperature to radiation changes, *Nat. Geosci.*, 1, 735–743, doi:10.1038/ngeo337, 2008.

Knutti, R. and Sedlacek, J.: Robustness and uncertainties in the new CMIP5 climate model projections, *Nat. Clim. Change*, doi:10.1038/nclimate1716, 2012.

Lindsay, K., Bonan, G. B., Doney, S.C, Hoffmann, F. M., Lawrence, D. M., Long, M. C., Mahowald, N. M., Moore, J. K., Randerson, J. T., and Thornton, P. E.: Preindustrial control and 20th century carbon cycle experiments with the earth system model CESM1-(BGC), *J. Climate*, submitted, 2013.

Meehl, G. A., Stocker, T. F., Collins, W. D., Friedlingstein, P., Gaye, A. T., Gregory, J. M., Kitoh, A., Knutti, R., Murphy, J. M., Noda, A., Raper, S. C. B., Watterson, I. G., Weaver, A. J., and Zhao, Z.-C.: *Climate Change 2007: The Physical Science Basis. Contribution of Working Group I to the Fourth Assessment Report of the Intergovernmental Panel on Climate Change*, chap. Global Climate Projections, Cambridge University Press, Cambridge, UK and New York, NY, USA, 747–846, 2007.

Metzger, R., Sartoris, F. J., Langenbuch, M., and Pörtner, H. O.: Influence of elevated CO<sub>2</sub> concentrations on thermal tolerance of the edible crab cancer pagurus, *J. Therm. Bio.*, 32, 144–151, doi:10.1016/j.jtherbio.2007.01.010, 2007.

## Multiple stressors of ocean ecosystems in the 21st century

L. Bopp et al.

Title Page

Abstract

Introduction

Conclusions

References

Tables

Figures

◀

▶

◀

▶

Back

Close

Full Screen / Esc

Printer-friendly Version

Interactive Discussion

- Moore, J. K., Doney, S. C., Kleypas, J. A., Glover, D. M., and Fung, I. Y.: An intermediate complexity marine ecosystem model for the global domain, *Deep-Sea Res. Pt. II*, 49, 403–462, doi:10.1016/S0967-0645(01)00108-4, 2002.
- Moore, J. K., Doney, S. C., and Lindsay, K.: Upper ocean ecosystem dynamics and iron cycling in a global 3-D model, *Global Biogeochem. Cy.*, 18, GB4028, doi:10.1029/2004GB002220, 2004.
- Moss, R. H., Edmonds, J. A., Hibbard, K. A., Manning, M. R., Rose, S. K., van Vuuren, D. P., Carter, T. R., Emori, S., Kainuma, M., Kram, T., Meehl, G. A., Mitchell, J. F. B., Nakicenovic, N., Riahi, K., Smith, S. J., Stouffer, R. J., Thomson, A. M., Weyant, J. P., and Wilbanks, T. J.: The next generation of scenarios for climate change research and assessment, *Nature*, 463, 747–756, 2010.
- Nixon, S. and Thomas, A.: On the size of the Peru upwelling ecosystem, *Deep-Sea Res Pt. I*, 48, 2521–2528, 2001.
- Orr, J. C.: Future changes in ocean carbonate chemistry in: *Ocean Acidification*, edited by: Gattuso, J.-P. and Hansson, L., Oxford University Press, 2011.
- Orr, J., Fabry, V., Aumont, O., Bopp, L., Doney, S., Feely, R., Gnanadesikan, A., Gruber, N., Ishida, A., Joos, F., Key, R., Lindsay, K., Maier-Reimer, E., Matear, R., Monfray, P., Mouchet, A., Najjar, R., Plattner, G., Rodgers, K., Sabine, C., Sarmiento, J., Schlitzer, R., Slater, R., Totterdell, I., Weirig, M., Yamanaka, Y., and Yool, A.: Anthropogenic ocean acidification over the twenty-first century and its impact on calcifying organisms, *Nature*, 437, 681–686, 2005.
- Oschlies, A., Schulz, K. G., Riebesell, U., and Schmittner, A.: Simulated 21st century's increase in oceanic suboxia by CO<sub>2</sub>-enhanced biotic carbon export, *Global Biogeochem. Cy.*, 22, GB4008, doi:10.1029/2007GB003147, 2008.
- Palmer, J. R. and Totterdell, I. J.: Production and export in a global ecosystem model, *Deep-Sea Res. Pt. I*, 48, 1169–1198, 2001.
- Patara L., Vichi, M., and Masina, S.: Impacts of natural and anthropogenic climate variations on North Pacific plankton in an Earth System Model, *Ecol. Model.*, 244, 132–147, doi:10.1016/j.ecolmodel.2012.06.012, 2012.
- Paulmier, A. and Ruiz-Pino, D.: Oxygen minimum zones (OMZs) in the modern ocean, *Prog. Oceanogr.*, 80, 113–128, 2009.
- Pauly, D. and Christensen, V.: Primary production required to sustain global fisheries, *Nature*, 374, 255–257, 1995.

## Multiple stressors of ocean ecosystems in the 21st century

L. Bopp et al.

[Title Page](#)

[Abstract](#)

[Introduction](#)

[Conclusions](#)

[References](#)

[Tables](#)

[Figures](#)

[◀](#)

[▶](#)

[◀](#)

[▶](#)

[Back](#)

[Close](#)

[Full Screen / Esc](#)

[Printer-friendly Version](#)

[Interactive Discussion](#)



Plattner, G., Joos, F., and Stocker, T.: Revision of the global carbon budget due to changing air-sea oxygen fluxes, *Global Biogeochem. Cy.*, 16, 1096–1108, doi:10.1029/2001GB001746, 2002.

Polovina, J. J., Howell, E. A., and Abecassis, M.: Ocean's least productive waters are expanding, *Geophys. Res. Lett.*, 35, L03618, doi:10.1029/2007GL031745, 2008.

Pörtner, H. O.: Ecosystem effects of ocean acidification in times of ocean warming: a physiologist's view, *Mar. Ecol. Prog. Ser.*, 373, 203–217, 2008.

Pörtner, H. O.: Oxygen and capacity limitation of thermal tolerance: a matrix for integrating climate related stressors in marine ecosystems, *J. Exp. Bio.*, 213, 881–893, hdl:10013/epic.34353, 2010.

Pörtner, H. O. and Knust, R.: Climate change affects marine fishes through the oxygen limitation of thermal tolerance, *Science*, 315, 95–97, doi:10.1126/science.1135471, 2007.

Pörtner, H. O., Langenbuch, M., and Michaelidis, B.: Synergistic effects of temperature extremes, hypoxia, and increases in CO<sub>2</sub> on marine animals: from Earth history to global change, *J. Geophys. Res.*, 110, C09S10, doi:10.1029/2004JC002561, 2004.

Resplandy, L., Bopp L., Orr, J. C., and Dunne J. P.: Role of mode and intermediate waters in future ocean acidification: analysis of CMIP5 models, *Geophys. Res. Lett.*, submitted, 2013.

Rykaczewski, R. R. and Dunne, J. P.: Enhanced nutrient supply to the California Current Ecosystem with global warming and increased stratification in an earth system model, *Geophys. Res. Lett.*, 37, L21606, doi:10.1029/2010GL045019, 2010.

Rykaczewski, R. R. and Dunne, J. P.: A measured look at ocean chlorophyll trends, *Nature*, 472, E5–E6, doi:10.1038/nature09952, 2011.

Riebesell, U., Schulz, K. G., Bellerby, R. G. J., Botros, M., Fritsche, P., Meyerhofer, M., Neill, C., Nondal, G., Oschlies, A., Wohlers, J., and Zollner, E.: Enhanced biological carbon consumption in a high CO<sub>2</sub> ocean, *Nature*, 450, 545–548, 2007.

Sabine, C. L., Feely, R. A., Gruber, N., Key, R. M., Lee, K., Bullister, J. L., Wanninkhof, R., Wong, C. S., Wallace, D. W. R., Tilbrook, B., Millero, F. J., Peng, T.-H., Kozyr, A., Ono, T., and Rios, A. F.: The oceanic sink for anthropogenic CO<sub>2</sub>, *Science*, 305, 367–371, 2004.

Sallée, J. B., Shuckburgh, E., Bruneau, N., Meijers, A., Wang, Z., and Bracegirdle, T.: Assessment of Southern Ocean water mass circulation in CMIP5 models: historical bias and forcing response, *J. Geophys. Res.*, submitted, 2012.

Sarmiento, J. L., Hughes, T. M. C., Stouffer, R. J., and Manabe, S.: Simulated response of the ocean carbon cycle to anthropogenic climate warming, *Nature*, 393, 245–249, 1998.

## Multiple stressors of ocean ecosystems in the 21st century

L. Bopp et al.

Title Page

Abstract

Introduction

Conclusions

References

Tables

Figures

◀

▶

◀

▶

Back

Close

Full Screen / Esc

Printer-friendly Version

Interactive Discussion



Schmittner, A., Oschlies, A., Matthews, H. D., and Galbraith, E. D.: Future changes in climate, ocean circulation, ecosystems, and biogeochemical cycling simulated for a business-as-usual CO<sub>2</sub> emission scenario until year 4000 AD, *Global Biogeochem. Cy.*, 22, GB1013, doi:10.1029/2007GB002953, 2008.

5 Steinacher, M., Joos, F., Frölicher, T. L., Plattner, G.-K., and Doney, S. C.: Imminent ocean acidification in the Arctic projected with the NCAR global coupled carbon cycle-climate model, *Biogeosciences*, 6, 515–533, doi:10.5194/bg-6-515-2009, 2009.

Steinacher, M., Joos, F., Frölicher, T. L., Bopp, L., Cadule, P., Cocco, V., Doney, S. C., Gehlen, M., Lindsay, K., Moore, J. K., Schneider, B., and Segschneider, J.: Projected 21st century decrease in marine productivity: a multi-model analysis, *Biogeosciences*, 7, 979–1005, doi:10.5194/bg-7-979-2010, 2010.

Stendardo, I. and Gruber, N.: Oxygen trends over five decades in the North Atlantic, *J. Geophys. Res.*, 117, C11004, doi:10.1029/2012JC007909, 2012.

15 Stramma, L., Johnson, G. C., Sprintall, J., and Mohrholz, V.: Expanding oxygen-minimum zones in the tropical oceans, *Science*, 320, 655–658, doi:10.1126/science.1153847, 2008.

Stramma, L., Oschlies, A., and Schmidtko, S.: Anticorrelated observed and modeled trends in dissolved oceanic oxygen over the last 50 years, *Biogeosciences Discuss.*, 9, 4595–4626, doi:10.5194/bg-9-4595-2012, 2012.

20 Szopa, S., Balkanski, Y., Schulz, M., Bekki, S., Cugnet, D., Fortems-Cheiney, A., Turquety, S., Cozic, A., Déandreis, C., Hauglustaine, D., Idelkadi, A., Lathièrre, J., Lefevre, F., Marchand, M., Vuolo, R., Yan, N., and Dufresne, J.-L.: Aerosol and ozone changes as forcing for climate evolution between 1850 and 2100, *Clim. Dynam.*, doi:10.1007/s00382-012-1408-y, 2012.

Takatani, Y., Sasano, D., Nakano, T., Midorikawa, T., and Ishii, M.: Decrease of dissolved oxygen after the mid-1980s in the western North Pacific subtropical gyre along the 137° E repeat section, *Global Biogeochem Cy.*, 26, GB2013, doi:10.1029/2011GB004227, 2012.

25 Taylor, K. E.: Summarizing multiple aspects of model performance in a single diagram, *J. Geophys. Res.*, 106, 7183–7192, 2001.

Taylor, K. E., Stouffer, R. J., and Meehl, G. A.: An overview of CMIP5 and the experiment design, *B. Am. Meteorol. Soc.*, 93, 485–498, doi:10.1175/BAMS-D-11-00094.1, 2012.

30 Thomas, M. K., Kremer, C. T., Klausmeier, C. A., and Litchman, E.: A global pattern in thermal adaptation in marine phytoplankton, *Science*, 338, 1085–1088, doi:10.1126/science.1224836, 2012.

---

## Multiple stressors of ocean ecosystems in the 21st century

L. Bopp et al.

---

Title Page

Abstract

Introduction

Conclusions

References

Tables

Figures

◀

▶

◀

▶

Back

Close

Full Screen / Esc

Printer-friendly Version

Interactive Discussion



Tagliabue, A., Bopp, L., and Gehlen, M.: The response of marine carbon and nutrient cycles to ocean acidification: large uncertainties related to phytoplankton physiological assumptions, *Global Biogeochem. Cy.*, 25, GB3017, doi:10.1029/2010GB003929, 2011.

5 Taucher, J. and Oschlies, A.: Can we predict the direction of marine primary production change under global warming?, *Geophys. Res. Lett.*, 38, L02603, doi:10.1029/2010GL045934, 2011.

10 van Vuuren, D. P., Edmonds, J., Kainuma, M., Riahi, K., Thomson, A., Hibbard, K., Hurtt, G. C., Kram, T., Krey, V., Lamarque, J.-F., Masui, T., Meinshausen, M., Nakicenovic, N., Smith, S. J., and Rose, S. K.: The representative concentration pathways: an overview, *Climatic Change*, 109, 5–31, doi:10.1007/s10584-011-0148-z, 2011.

Vichi M., Pinardi, N., and Masina, S.: A generalized model of pelagic biogeochemistry for the global ocean ecosystem. Part I: Theory, *J. Marine Syst.*, 64, 89–109, doi:10.1016/j.jmarsys.2006.03.006, 2007.

15 Vichi, M., Manzini, E., Fogli, P. G., Alessandri, A., Patara, L., Scoccimarro, E., Masina, S., and Navarra, A.: Global and regional ocean carbon uptake and climate change: sensitivity to a substantial mitigation scenario, *Clim. Dynam.*, 37, 1929–1947, doi:10.1007/s00382-011-1079-0, 2011.

20 Yamamoto, A., Kawamiya, M., Ishida, A., Yamanaka, Y., and Watanabe, S.: Impact of rapid sea-ice reduction in the Arctic Ocean on the rate of ocean acidification, *Biogeosciences*, 9, 2365–2375, doi:10.5194/bg-9-2365-2012, 2012.

## Multiple stressors of ocean ecosystems in the 21st century

L. Bopp et al.

**Table 1.** A brief description of the models used in this study, indicating atmospheric and oceanic resolution lev is the number of levels on the vertical, and then is indicated the horizontal resolution in degrees), the marine biogeochemical component included in the ESM, the number of explicit phytoplankton groups represented, and the different RCP scenarios performed and used in this study.

Model	Atmosphere	Ocean	Ref.	MBG	Phytoplankton	Ref.	RCPs
CESM1-BGC	26 lev. 1.25°/0.94°	60 lev. 1.125°/0.27° –0.53°	Gent et al. (2011), Lindsay et al. (2013)	BEC	3 (diatom, nanophyto, diazotroph)	Moore et al. (2004), Doney et al. (2009)	8.5, 4.5
CMCC-ESM	39 lev, 3.8°	31 lev. 0.5–2°	Vichi et al. (2011), Cagnazzo et al. (2013)	PELAGOS	3 (diatoms, flagellates, picophytoplankton)	Vichi et al. (2007)	8.5
GFDL-ESM2G	24 lev., 2.5°/2.0°	63 lev., 0.3–1°	Dunne et al. (2012a)	TOPAZ2	3 (large separated into diatoms and non-diatom, small cyanobacteria, diazotroph)	Dunne et al. (2012b)	8.5, 6.0, 4.5 and 2.6
GFDL-ESM2M	24 lev., 2.5°/2.0°	50 lev., 0.3–1°	Dunne et al. (2012a)	TOPAZ2	3 (large separated into diatoms and non-diatom, small cyanobacteria, diazotroph)	Dunne et al. (2012b)	8.5, 6.0, 4.5 and 2.6
HadGEM2-ES	38 lev., 1.2°/1.9°	40 lev., 0.3–1°	HadGEM2 Team (2011), Collins et al. (2011)	Diat- HadOCC	2 (diatom, non-diatom)	Palmer and Totterdell, (2000)	8.5, 6.0, 4.5 and 2.6
IPSL-CM5A-LR	39 lev, 1.9°/3.8°	31 lev. 0.5–2°	Dufresne et al. (2013)	PISCES	2 (diatoms and nanophyto)	Aumont and Bopp (2006), Séférian et al. (2012)	8.5, 6.0, 4.5 and 2.6
IPSL-CM5A-MR	39 lev, 1.2°/2.5°	31 lev. 0.5–2°	Dufresne et al. (2013)	PISCES	2 (diatoms and nanophyto)	Aumont and Bopp (2006), Séférian et al. (2012)	8.5, 4.5 and 2.6
MPI-ESM-LR	47 lev, 1.9°	40 lev, 1.5°	Giorgetta et al., (2013)	HAMOCC5.2	1 (but separated into diatoms and calcifiers)	Ilyina et al. (2013)	8.5, 4.5 and 2.6
MPI-ESM-MR	95 lev, 1.9°	40 lev, 0.4°	Giorgetta et al., (2013)	HAMOCC5.2	1 (but separated into diatoms and calcifiers)	Ilyina et al. (2013)	8.5, 4.5 and 2.6
NorESM1-ME	26 lev, 1.9°/2.5°	53 lev, 1°	Bentsen et al. (2012)	HAMOCC5.1	1 (but separated into diatoms and calcifiers)	Assmann et al. (2010)	8.5, 6.0, 4.5 and 2.6

Title Page

Abstract

Introduction

Conclusions

References

Tables

Figures

◀

▶

◀

▶

Back

Close

Full Screen / Esc

Printer-friendly Version

Interactive Discussion



## Multiple stressors of ocean ecosystems in the 21st century

L. Bopp et al.

**Table 2.** Observed and modeled present-day global average of sea surface temperature ( $^{\circ}\text{C}$ ), surface pH (pH unit), dissolved oxygen ( $\text{mmol m}^{-3}$ ), volumes of waters ( $10^{15} \text{ m}^3$ ) in which  $\text{O}_2$  is less than 80, 50 and 5  $\text{mmol m}^{-3}$ , net primary productivity ( $\text{PgCyr}^{-1}$ ) and export production of organic particles at 100 m ( $\text{PgCyr}^{-1}$ ). Interannual standard deviations, when meaningful, are also indicated in parenthesis. Observed estimates are from Reynolds et al. (2008) for SST, computed using DIC and alkalinity from Key et al. (2004) for surface pH, from WOA (2009) for  $\text{O}_2$  content, from Bianchi et al. (2012) for the volumes of low oxygen waters, from Behrenfeld et al. (1997) for NPP. All data are from 1990–1999 except satellite-derived NPP from 1997–2006, and oxygen quantities from climatologies (n.a. = not available).

	SST	spH	$\text{O}_2$ content	vol 80	Vol 50	vol 5	PP (1990– 1999)	EXP
	$^{\circ}\text{C}$	(–)	$\text{mmol m}^{-3}$	$1 \times 10^{15} \text{ m}^3$	$1 \times 10^{15} \text{ m}^3$	$1 \times 10^{15} \text{ m}^3$	$\text{PgCyr}^{-1}$	$\text{PgCyr}^{-1}$
OBS	18.32	8.104	178	126	60.4	2.43	52.10	
MODEL:								
CESM1-BGC	18.682 (0.13)	8.085 (0.004)	190	133.40	79.31	16.43	54.45 (0.25)	7.70 (0.08)
CMCC-ESM	18.211 (0.09)	8.053 (0.003)	201	34.13	20.79	6.22	33.34 (1.07)	n.a
GFDL-ESM2G	18.098 (0.13)	8.095 (0.004)	184	166.99	115.73	50.45	63.76 (0.37)	4.95 (0.02)
GFDL-ESM2M	18.536 (0.12)	8.091 (0.004)	169	166.80	108.73	34.17	78.71 (0.51)	7.39 (0.1)
HadGEM2-ES	18.002 (0.07)	8.105 (0.004)	176	54.20	16.90	0.41	35.30 (0.48)	5.40 (0.07)
IPSL-CM5A-LR	17.279 (0.12)	8.082 (0.004)	148	258.95	12.50	0.79	30.90 (0.29)	6.61 (0.09)
IPSL-CM5A-MR	17.760 (0.13)	8.082 (0.004)	136	363.33	225.68	2.38	33.34 (0.40)	7.01 (0.09)
MPI-ESM-LR	17.899 (0.19)	8.093 (0.004)	173	167.55	107.12	51.41	56.64 (1.69)	8.09 (0.27)
MPI-ESM-MR	18.220 (0.11)	8.091 (0.005)	172	188.97	121.26	46.72	52.52 (1.49)	7.42 (0.21)
NorESM1-ME	17.688 (0.10)	8.088 (0.004)	231	111.01	84.47	48.07	40.60 (0.91)	7.93 (0.18)

Title Page

Abstract

Introduction

Conclusions

References

Tables

Figures

◀

▶

◀

▶

Back

Close

Full Screen / Esc

Printer-friendly Version

Interactive Discussion



## Multiple stressors of ocean ecosystems in the 21st century

L. Bopp et al.

**Table 3.** Evolution of SST, pH, global O<sub>2</sub>, integrated NPP for all models and all scenarios. Model means in 2090–2099 (compared to 1990–1999) and inter-model standard deviations in 2090–2099.

	RCP8.5		RCP6.0		RCP4.5		RCP2.6
	Change	Std	Change	Std	Change	Std	Change
SST (°C)	2.73	0.72	1.58	0.48	1.28	0.56	0.71
Surface pH (–)	–0.33	0.003	–0.22	0.002	–0.15	0.001	–0.07
O <sub>2</sub> content (%)	–3.45	0.44	–2.57	0.39	–2.37	0.30	–1.81
Integrated NPP (%)	–8.6	7.9	–3.9	5.7	–3.6	5.7	–2.0

Title Page

Abstract

Introduction

Conclusions

References

Tables

Figures

◀

▶

◀

▶

Back

Close

Full Screen / Esc

Printer-friendly Version

Interactive Discussion



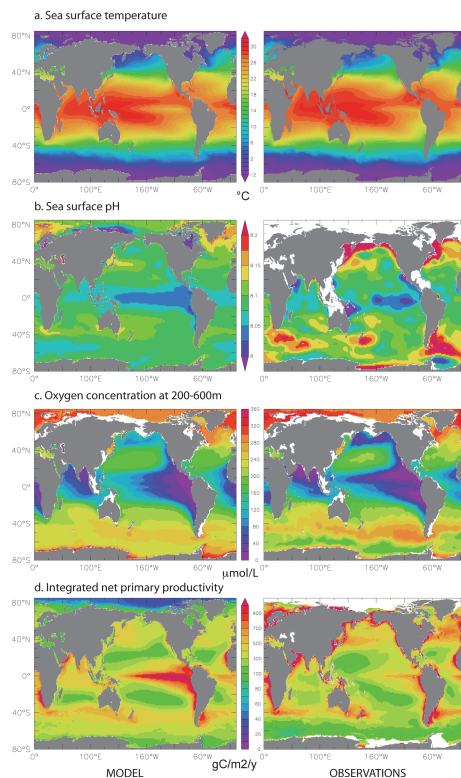


**Fig. 1.** Comparison of model-mean **(a)** SST ( $^{\circ}\text{C}$ ), **(b)** surface pH (pH unit), **(c)** sub-surface  $\text{O}_2$  averaged over 200–600 m ( $\text{mmol m}^{-3}$ ), and **(d)** vertically integrated PP ( $\text{g C m}^{-2} \text{yr}^{-1}$ ) with data-based products. Observed estimates are from Reynolds et al. (2008) for SST, computed using DIC and alkalinity from Key et al. (2004) for surface pH, from WOA (2009) for  $\text{O}_2$ , from Behrenfeld et al. (1997) for NPP. All data are from 1990–1999 except observed NPP from 1997–2006, and  $\text{O}_2$  concentration from WOA 2009 climatology.

**Multiple stressors of ocean ecosystems in the 21st century**

L. Bopp et al.

[Title Page](#)

<a href="#">Abstract</a>	<a href="#">Introduction</a>
<a href="#">Conclusions</a>	<a href="#">References</a>
<a href="#">Tables</a>	<a href="#">Figures</a>

⏪
⏩

◀
▶

<a href="#">Back</a>	<a href="#">Close</a>
----------------------	-----------------------

[Full Screen / Esc](#)

[Printer-friendly Version](#)

[Interactive Discussion](#)



## Multiple stressors of ocean ecosystems in the 21st century

L. Bopp et al.

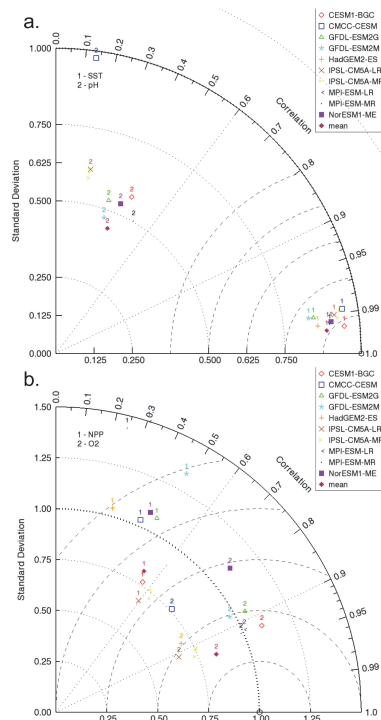


**Fig. 2.** Taylor diagrams showing the correspondence between model results and observations for **(a)** annual-mean SST and annual-mean surface pH, and **(b)** annual mean sub-surface  $O_2$  averaged over 200–600 m and annual-mean vertically integrated NPP. Data-based products are from Reynolds et al. (2008) for SST, computed using DIC and alkalinity from Key et al. (2004) for surface pH, from WOA (2009) for dissolved  $O_2$  concentrations, from Behrenfeld et al. (1997) for NPP. All data are from 1990–1999 except observed NPP from 1997–2006, and  $O_2$  concentration from WOA 2009 climatology. The angular coordinate indicates the correlation coefficient ( $R$ ), the radial coordinate shows the normalised standard deviation ( $\text{stdmodel}/\text{stdobs}$ ). A model perfectly matching the observations would reside in point (1,1).

Title Page

Abstract

Introduction

Conclusions

References

Tables

Figures



Back

Close

Full Screen / Esc

Printer-friendly Version

Interactive Discussion



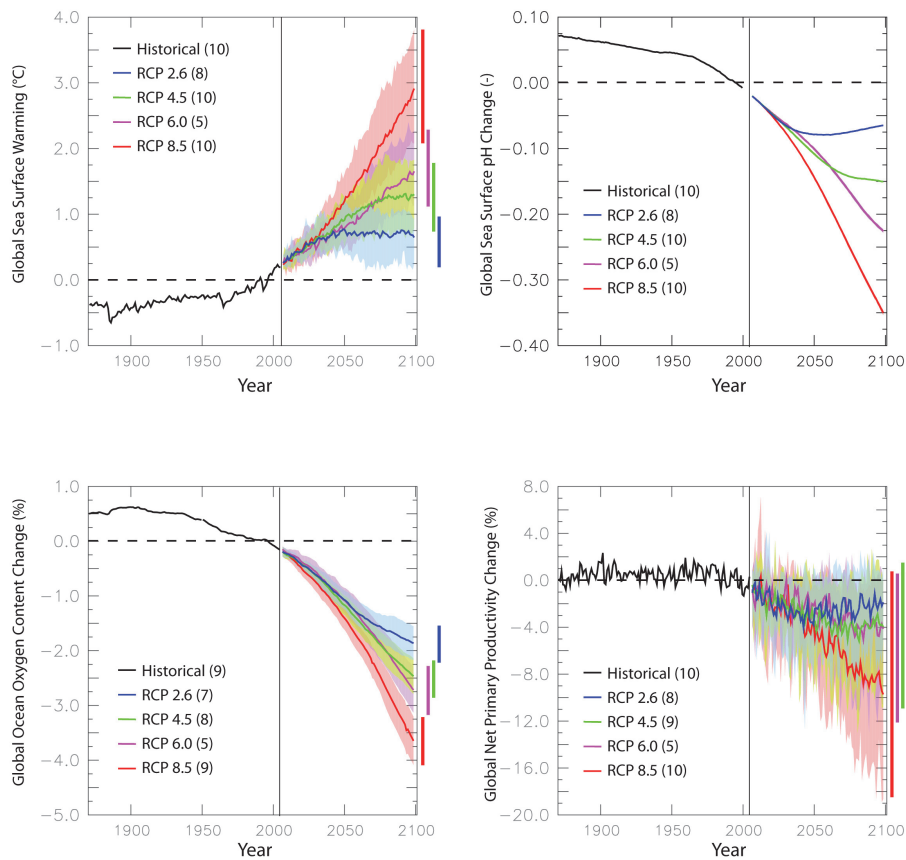


**Fig. 3.** Model-mean time series of global sea surface warming (°C), surface pH change (pH unit), ocean O<sub>2</sub> content change (%), and global NPP change (%) over 1870–2100 using historical simulations as well as all RCPs simulations. Shading indicates one inter-model standard deviation. All variables are plotted relative to 1990–1999.

**Multiple stressors of ocean ecosystems in the 21st century**

L. Bopp et al.

[Title Page](#)

[Abstract](#)   [Introduction](#)

[Conclusions](#)   [References](#)

[Tables](#)   [Figures](#)

[◀](#)   [▶](#)

[◀](#)   [▶](#)

[Back](#)   [Close](#)

[Full Screen / Esc](#)

[Printer-friendly Version](#)

[Interactive Discussion](#)



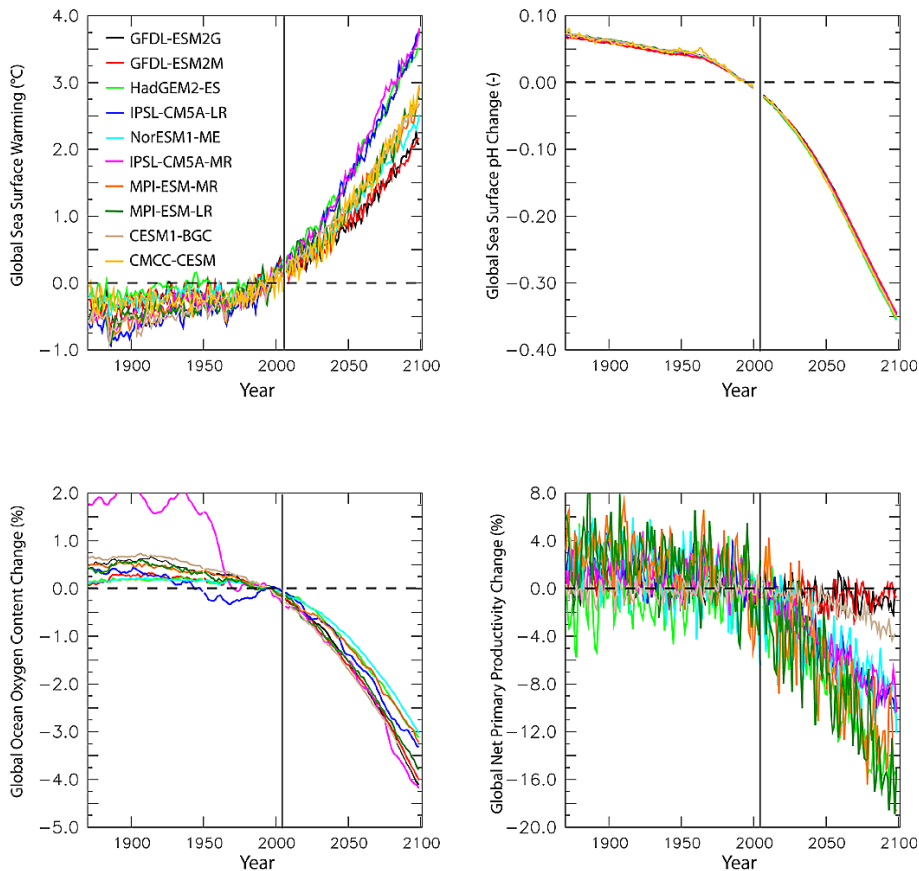


**Fig. 4.** Individual model time series of global sea surface warming ( $^{\circ}\text{C}$ ), surface pH change (pH unit), ocean  $\text{O}_2$  content change (%), and global NPP change (%) over 1870–2100 using historical simulations as well as all RCP8.5 simulations.

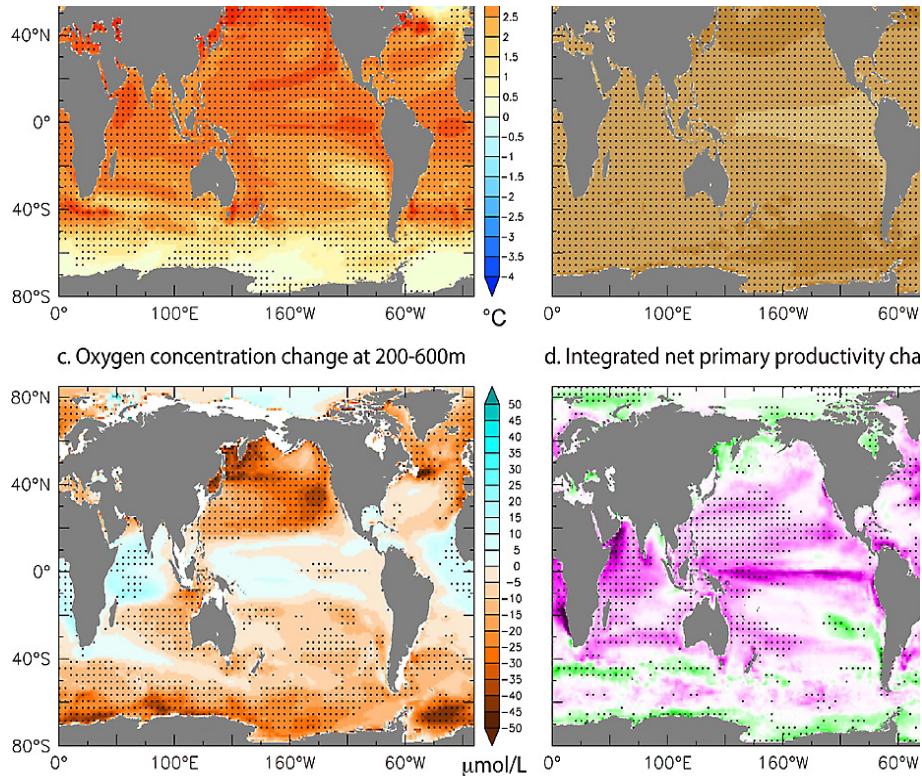


**Fig. 5.** Change in stressor intensity in 2090–2099 relative to 1990–1999 under RCP8.5. Multi-model mean of **(a)** sea surface warming ( $^{\circ}\text{C}$ ), **(b)** surface pH change (pH unit), **(c)** sub-surface dissolved  $\text{O}_2$  concentrations change (averaged between 200 m and 600 m,  $\text{mmol m}^{-3}$ ), and **(d)** vertically integrated NPP ( $\text{gCm}^{-2}\text{yr}^{-1}$ ). Stippling marks high robustness. Robustness is estimated from inter-model standard deviation for SST and pH, from agreement on sign of changes for  $\text{O}_2$  and NPP. Dark red color shading is used to mark the change in stressor that is detrimental for the marine environment.

Multiple stressors of ocean ecosystems in the 21st century

L. Bopp et al.

Title Page

Abstract

Introduction

Conclusions

References

Tables

Figures

◀

▶

◀

▶

Back

Close

Full Screen / Esc

Printer-friendly Version

Interactive Discussion



## Multiple stressors of ocean ecosystems in the 21st century

L. Bopp et al.

Title Page

Abstract

Introduction

Conclusions

References

Tables

Figures



Back

Close

Full Screen / Esc

Printer-friendly Version

Interactive Discussion

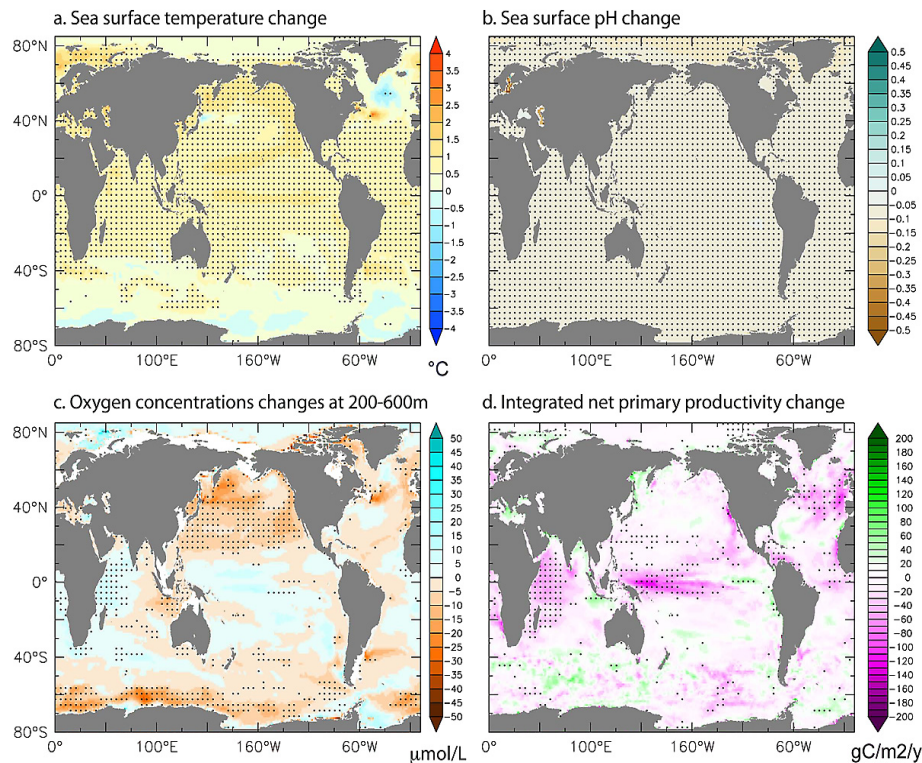


**Fig. 6.** Change in stressor intensity in 2090–2099 relative to 1990–1999 under RCP2.6. Multi-model mean of **(a)** sea surface warming ( $^{\circ}\text{C}$ ), **(b)** surface pH change (pH unit), **(c)** sub-surface dissolved  $\text{O}_2$  concentrations change (averaged between 200 m and 600 m,  $\text{mmol m}^{-3}$ ), and **(d)** vertically integrated NPP ( $\text{gC m}^{-2} \text{yr}^{-1}$ ). Stippling marks high robustness. Robustness is estimated from inter-model standard deviation for SST and pH, from agreement on sign of changes for  $\text{O}_2$  and NPP.

## Multiple stressors of ocean ecosystems in the 21st century

L. Bopp et al.

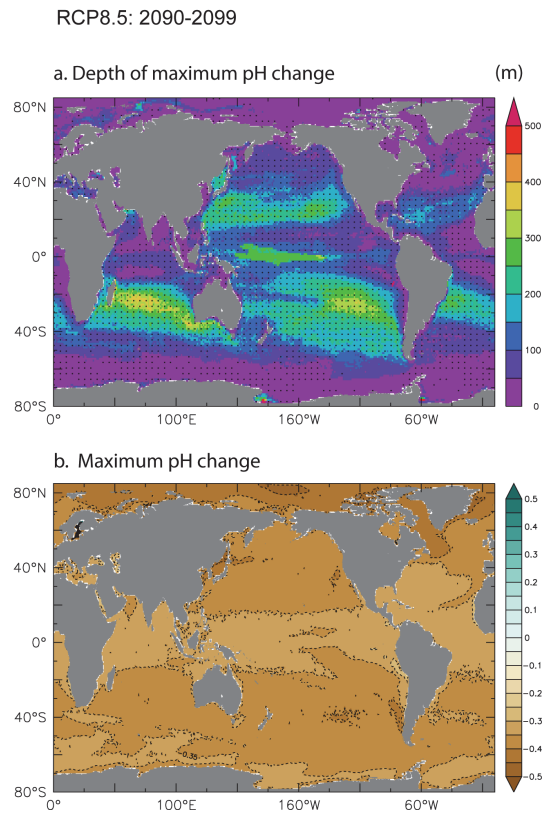


**Fig. 7.** Change in pH in 2090–2099 relative to 1990–1999 under RCP8.5. **(a)** Model-mean depth of the maximum changes in pH. Robustness estimated from inter-model standard deviation and **(b)** model-mean changes of pH at that depth.

Title Page

Abstract

Introduction

Conclusions

References

Tables

Figures

◀

▶

◀

▶

Back

Close

Full Screen / Esc

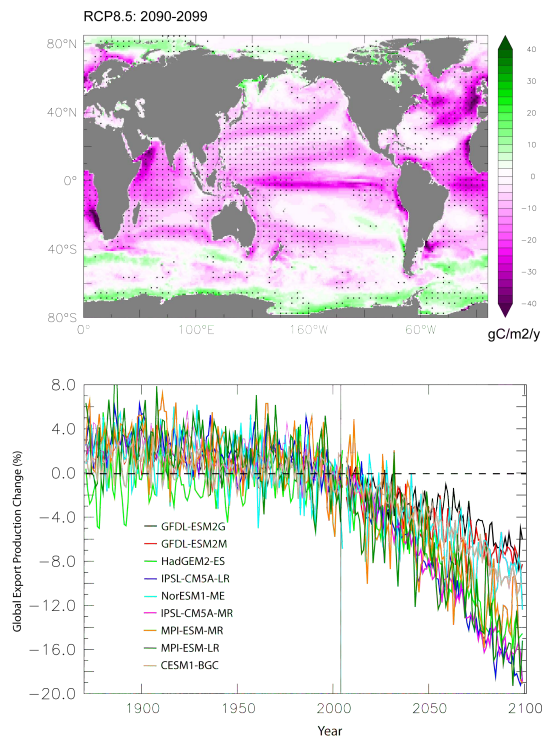
Printer-friendly Version

Interactive Discussion



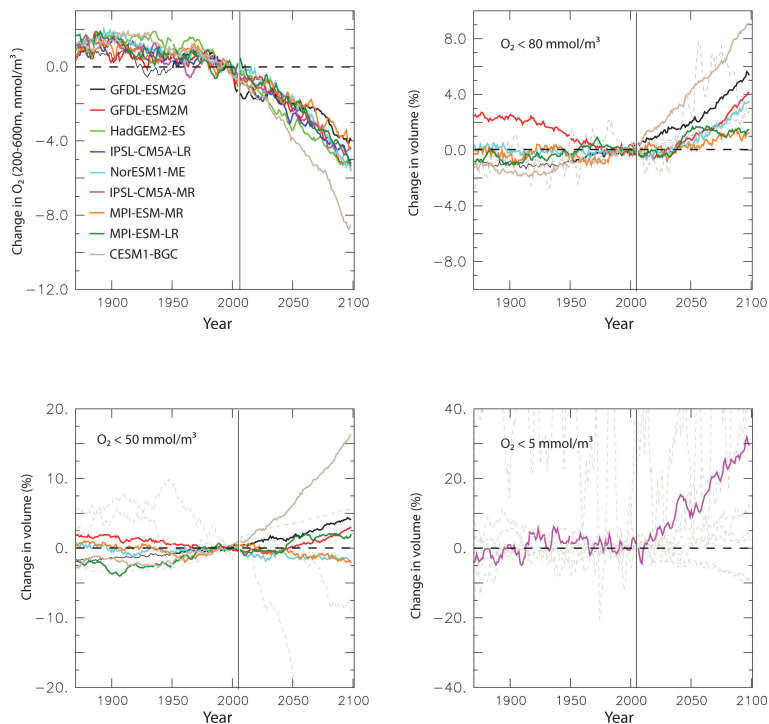
## Multiple stressors of ocean ecosystems in the 21st century

L. Bopp et al.



**Fig. 8.** Change in export production of organic particles at 100 m under RCP8.5. **(a)** Multi-model mean change of export production in 2090–2099 relative to 1990–1999 (%). Stippling marks robustness from agreement on sign of changes. **(b)** Time series for all models of the change of export production relative to 1990–1999 (%) from 1870 to 2099 using historical and RCP8.5 simulations.

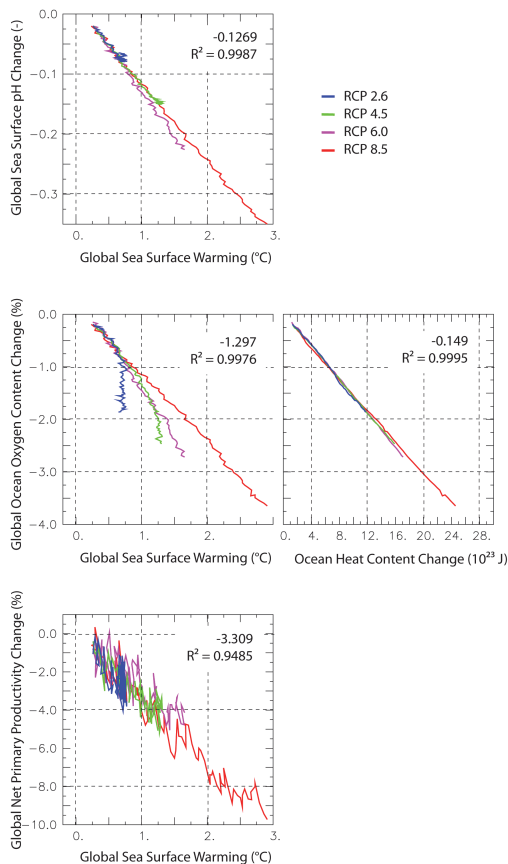
[Title Page](#)
[Abstract](#)
[Introduction](#)
[Conclusions](#)
[References](#)
[Tables](#)
[Figures](#)
[Back](#)
[Close](#)
[Full Screen / Esc](#)
[Printer-friendly Version](#)
[Interactive Discussion](#)

**Fig. 9.** Individual model time series for RCP8.5 and for of all models of **(a)** sub-surface dissolved  $O_2$  concentrations changes between 200 and 600 m ( $\text{mmol m}^{-3}$ ), changes in (relative unit) volume with **(b)**  $O_2 < 80 \text{ mmol m}^{-3}$ , **(c)**  $O_2 < 50 \text{ mmol m}^{-3}$ , **(d)**  $O_2 < 5 \text{ mmol m}^{-3}$  (as in Cocco et al., 2012). Only models that simulate volumes “close” (in between +100 % and -50 % of the data-based estimated volume) to the ones estimated with WOA-corrected oxygen climatology (Bianchi et al., 2012) are colored.

## Multiple stressors of ocean ecosystems in the 21st century

L. Bopp et al.



**Fig. 10.** Relations between model-mean changes in surface pH (pH unit), global O<sub>2</sub> content (%) and global NPP and model-mean sea surface warming (°C) for all scenarios. For global O<sub>2</sub> content, changes are also plotted against changes in total heat content (10<sup>22</sup>J). All changes are relative to 1990–1999 and plotted over 2006–2100.

[Title Page](#)
[Abstract](#)
[Introduction](#)
[Conclusions](#)
[References](#)
[Tables](#)
[Figures](#)
[Back](#)
[Close](#)
[Full Screen / Esc](#)
[Printer-friendly Version](#)
[Interactive Discussion](#)


## Multiple stressors of ocean ecosystems in the 21st century

L. Bopp et al.

Title Page

Abstract

Introduction

Conclusions

References

Tables

Figures



Back

Close

Full Screen / Esc

Printer-friendly Version

Interactive Discussion

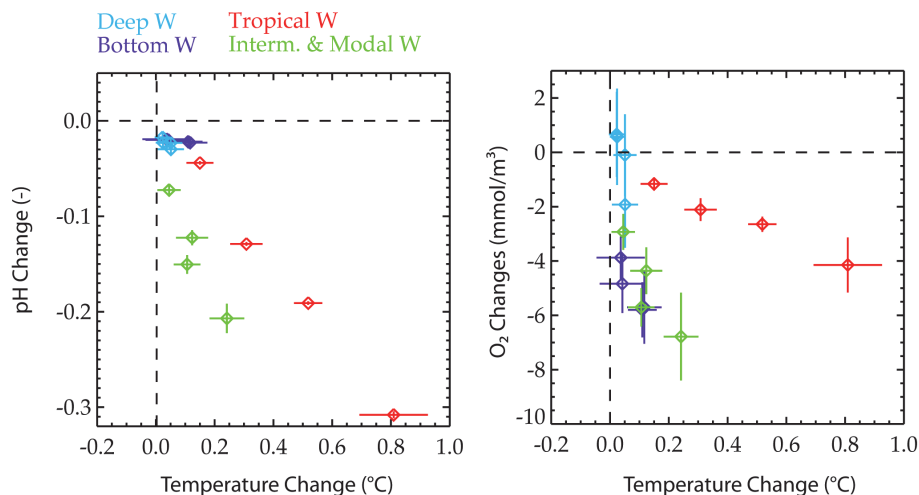


**Fig. 11.** Relations between model-mean changes in pH (pH unit), dissolved O<sub>2</sub> (mmol m<sup>-3</sup>) and model-mean temperature change (°C), in four distinct global water masses (tropical water mass, modal and intermediate water mass, deep water mass and bottom water mass). For a definition of the different water masses, please see Sect. 2.3. Inter-model standard deviations are also indicated.

## Multiple stressors of ocean ecosystems in the 21st century

L. Bopp et al.

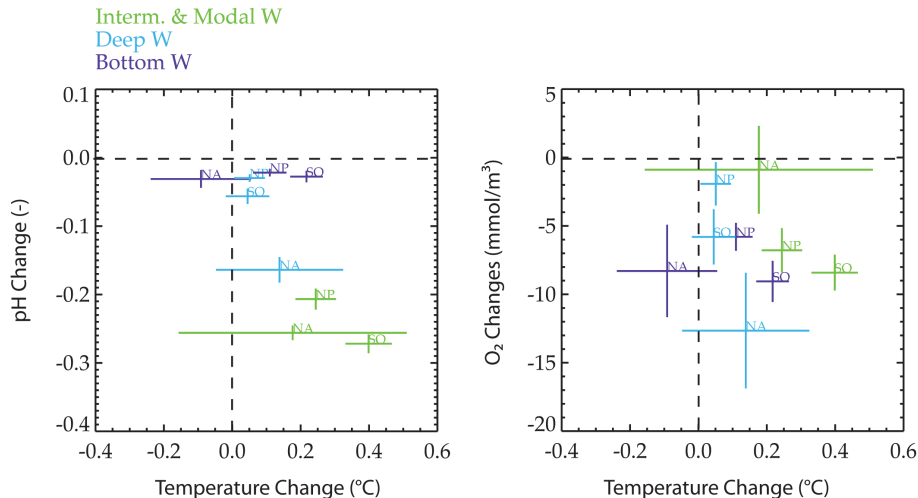


**Fig. 12.** Relation between model-mean changes in pH (pH unit), dissolved O<sub>2</sub> (mmol m<sup>-3</sup>) and model-mean temperature change (°C), in three distinct global water masses (modal and intermediate water mass, deep water mass and bottom water mass) and for 3 different basins (North Atlantic, North Pacific and Southern Ocean). For a definition of the different water masses, please see Sect. 2.3. Inter-model standard deviations are also indicated.

Title Page

Abstract

Introduction

Conclusions

References

Tables

Figures

◀

▶

◀

▶

Back

Close

Full Screen / Esc

Printer-friendly Version

Interactive Discussion



## Multiple stressors of ocean ecosystems in the 21st century

L. Bopp et al.

RCP8.5 - 2090s, changed from 1990s

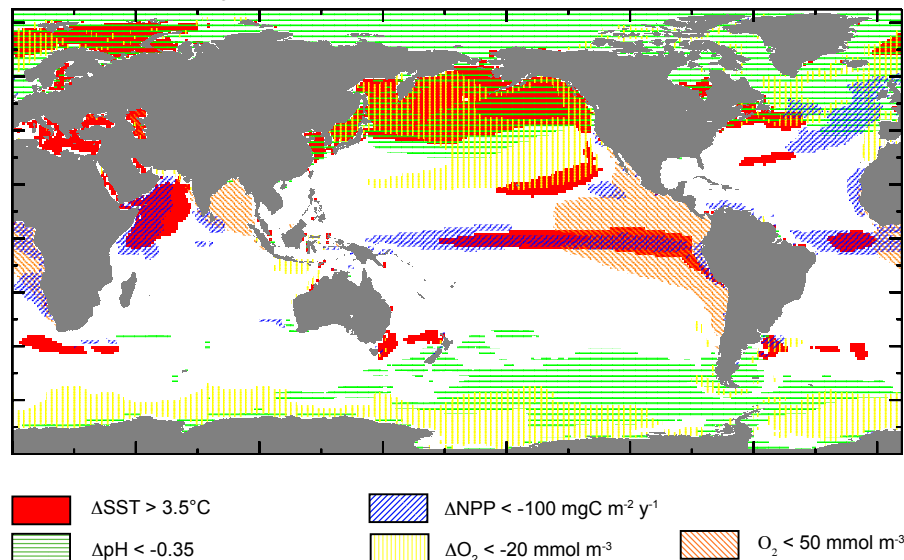


**Fig. 13.** Change in multiple stressor intensity in 2090–2099 relative to 1990–1999 under the RCP8.5 scenario. Red indicates where sea surface warming exceeds  $+3.5^\circ\text{C}$ , hatched green indicates where surface pH decreases by more than  $-0.35$  pH unit, hatched yellow indicates where sub-surface (200–600 m) oxygen concentrations decrease by more than  $20 \text{ mmol m}^{-3}$ , and hatched blue indicates where vertically integrated NPP decreases by more than  $100 \text{ gC m}^{-2} \text{ yr}^{-1}$ . In addition, hatched orange indicate present-day simulated low-oxygen ( $< 50 \text{ mmol m}^{-3}$ ) sub-surface (200–600 m) waters.

Title Page

Abstract

Introduction

Conclusions

References

Tables

Figures

◀

▶

◀

▶

Back

Close

Full Screen / Esc

Printer-friendly Version

Interactive Discussion

